REPORT DOCUMENTATION PAGE

Form Approved
OMB No. 074-0188

1. AGENCY USE ONLY (Leave blank)	2. REPORT DATE	3. REPORT TYPE AND DATES COVERED
	October 3, 2002	Final Technical (5/1/99-4/30/02)

4. TITLE AND SUBTITLE
Defect Reduction in GlGaN/GaN Ultra-Violet Photodetectors

5. FUNDING NUMBERS
Grant #N00014-00-1-0628

6. AUTHOR(S)
Hadis Morkoç, Ph.D.

7. PERFORMING ORGANIZATION NAME(S) AND ADDRESS(ES)

Virginia Commonwealth University
School of Engineering
PO Box 843068
Richmond, VA 23284-3068

8. PERFORMING ORGANIZATION REPORT NUMBER
Final Technical for #528467

9. SPONSORING / MONITORING AGENCY NAME(S) AND ADDRESS(ES)

Office of Naval Research
Program Officer Yoon S. Park
ONR Code 312
Ballston Center Tower One
800 N. Quincy St., Arlington, VA 22217

10. SPONSORING / MONITORING AGENCY REPORT NUMBER

11. SUPPLEMENTARY NOTES

12a. DISTRIBUTION / AVAILABILITY STATEMENT

APPROVED FOR PUBLIC RELEASE

12b. DISTRIBUTION CODE

Since the native substrates are not easily available in sufficient size and quantity, alternative methods by using various types of buffer layers to isolate the films from the deleterious effect of the substrate have been investigated. In the case of MOCVD, a thin GaN or AlN film grown at low temperature (~500 o C) is commonly used as the buffer layer for the active layer growth at much higher temperatures. The other buffer layers such as the low temperature InN layer on sapphire A-face, double low temperature AlN or GaN layers between high temperature grown GaN, GaN/AlGaN superlattices, and the SiO2 patterned GaN/AlN buffer on SiC substrate (the lateral growth) were all investigated to improve the epilayer quality. Recently, the effect of the growth rate, the thermal annealing, and the impurity doping of buffer layers were also reported. As compared to MOCVD growth, much fewer investigations were reported for MBE. In the latter case, an AlN buffer layer is commonly used as the buffer layer and a high growth temperature (~900 o C) may lead to a better epilayer quality. The nitridation temperature of sapphire substrate and the III/V flux ratio were found to have an impact on the GaN quality.

14. SUBJECT TERMS
Semiconductors, Nitrides, heterostructures, GaN, photodetectors

15. NUMBER OF PAGES
53

16. PRICE CODE

17. SECURITY CLASSIFICATION OF REPORT	18. SECURITY CLASSIFICATION OF THIS PAGE	19. SECURITY CLASSIFICATION OF ABSTRACT	20. LIMITATION OF ABSTRACT
Unclassified	Unclassified	Unclassified	SAR

Report for ONR#N00014-00-1-0628

Defect Reduction in AlGaN/GaN Ultra-Violet Photodetectors

TABLE OF CONTENTS

1. Introduction 1

2. Crystal growth 5

3. Formations and controllability of quantum dot density and size 10

4. Material characterization 16

5. Dislocation reduction using quantum dot buffer layer 22

6. Investigation of GaN/AlGaN MQW back-illuminated Schottky barrier UV photodetectors 30

7. Summary 39

8. Publication results from this grant 41

9. Biography of PI, Hadis Morkoç 44

1. Introduction

III-nitride semiconductors have wide applications in light emitting, detecting, and electronic devices and have been investigated very extensively in the last decade. GaN based light emitting devices (green, blue, violet) and laser (violet) diodes have been achieved using heterostructures and quantum wells. Recently, Temkin's group reported MQW in an effort to extend the range of wavelength in LED. The lack of appropriate substrates is a pending problem in the nitride device development, in general. III-nitride epilayers or quantum wells are commonly grown on foreign substrates by metalorganic chemical vapor deposition (MOCVD) and molecular beam epitaxy (MBE). Sapphire (α-Al_2O_3) substrates are most extensively used owing to their relatively low cost and large size. However, the large mismatches of lattice constant, thermal expansion coefficient, and stacking order of III-nitrides from substrates result in high defect density in the epilayers. Although the dislocation density near the GaN surface may decrease with the film thickness, the typical value for a GaN layers with thicknesses in the range of few to ten μm grown on sapphire substrate is still in the order of $10^9 cm^{-2}$ or higher. This value is too large as compared to $\sim 10^4 cm^{-2}$ in homoepitaxial GaAs films and definitely affects the electrical and optical properties as well as the device performance. The attempt to obtain high efficient true solar-blind photodetector is hindered by lower layer quality of AlGaN. Since the photodetectors work under very low currents and very low photon fluxes compared to other electronic and optoelectronic devices such as HEMTs, LEDs and LDs, they reflect even more pronouncedly some of the problems in AlGaN layer quality. Basically, the characteristics and limitations in present AlGaN photodetectors are directly dependent on the quality of the (Al,Ga)N epitaxial layers achieved today, i.e., the reduction of dislocation density.

Great strides have been made to grow GaN films with reduced defect density. One obvious method is to use native substrates. Thick GaN layers can be prepared by the technique such as hydride vapor phase epitaxy (HVPE) and can be used as the substrates (templates) for further growth. Using GaN substrates grown by the high-pressure technique, the dislocation density as low as $10^5 cm^{-2}$ has been reported in the GaN/AlGaN quantum well structures grown by MBE. The photoluminescence (PL) efficiency was greatly improved as compared to the heteroepitaxial materials. On GaN templates grown on sapphire by HVPE, an electron mobility of higher than 50000 cm^2/Vs was observed from two dimensional electron gas of density $2.8x10^{12} cm^{-2}$. In addition to the HVPE prepared substrate, thick GaN templates grown by MOCVD on sapphire can also be used as the substrate for MBE re-growth. A room temperature electron mobility of about 1200 cm^2/Vs was measured in a GaN film grown on such templates. The dislocation density of ~ $5x10^8 cm^{-2}$ was reported.

Since the native substrates are not easily available in sufficient size and quantity, alternative methods by using various types of buffer layers to isolate the films from the deleterious effect of the substrate have been investigated. In the case of MOCVD, a thin GaN or AlN film grown at low temperature (~500°C) is commonly used as the buffer layer for the active layer growth at much higher temperatures. The other buffer layers such as the low temperature InN layer on sapphire A-face, double low temperature AlN or GaN layers between high temperature grown GaN, GaN/AlGaN superlattices, and the SiO_2 patterned GaN/AlN buffer on SiC substrate (the lateral growth) were all investigated to improve the epilayer quality. Recently, the effect of the growth rate, the thermal annealing, and the impurity doping of buffer layers were also reported. As compared to MOCVD growth, much fewer investigations were reported for MBE. In the latter case, an AlN buffer layer is

commonly used as the buffer layer and a high growth temperature (~900 °C) may lead to a better epilayer quality. The nitridation temperature of sapphire substrate and the III/V flux ratio were found to have an impact on the GaN quality.

This report is organized as follows: After giving general information on routine substrate preparation and crystal growth of AlN/GaN buffer layers we will continue to present the report as composed of three parts to guide and follow the topics more easily; the first part contains the investigation of QDs layers grown on the AlN barrier layer spaced with 5nm AlN without cap layer. Formation and properties of QD layers were analyzed as a function of growth temperatures and pressure(III/V ratio) by using Atomic Force Microscopy (AFM). In the second part of this report we investigated the GaN crystal quality by utilizing a stack of quantum dots (QDs) as buffer layers. The GaN films grown on GaN/AlN buffer layers containing multiple QDs were characterized by x-ray diffraction (XRD), photoluminescence (PL), and defect delineate chemical etching, atomic force microscopy (AFM), and transmission electron microscopy (TEM). The results were also compared to those observed from the samples grown without using QDs as part of buffer layer. Third part consists of the experimental results of a novel visible-blind UV photodetector having GaN/AlGaN MQW in their active region. Schottky barrier types of MQW UV detectors were investigated experimentally with a proposed phenomenological model involved in carrier transport.

2 Crystal Growth

The samples being investigated were grown on c-plane sapphire substrates by molecular beam epitaxy. The as received sapphire substrates suffer from mechanical chemical polish damage. When the sapphires were directly used as substrates, a series of steps were taken to not only clean the sapphire surface, but also eliminate the damage. Sapphire substrates first undergo a chemical (solvent) cleaning procedure. This is followed by the substrate being dipped in a solution of TriChlorEtane (TCE) and kept at 300 °C, for 5 minutes. The substrate is then rinsed for 3 minutes each in acetone and methanol. This procedure is followed by a 3-minute rinse in deionized (DI) water. The above steps may be repeated three times to complete the degreasing process.

Following the degreasing procedure, the surface damage is removed by chemical etching. A 3:1 solution of hot H_2SO_4: H_3PO_4 (300 °C) is then used for 20 minutes to remove some of the surface material. This is followed by a rinse in DI water for 5 minutes. This procedure serves to remove the very surface damage but does not lead to smooth surfaces. To remove the scratches and other deeper damage, sapphire substrates were subjected to a high temperature heat-treatment in air (about 1400 ° C) and for one hour. Sapphire substrates subjected to this high temperature heat treatment exhibit very smooth morphology as determined by atomic force microscopy (AFM) images. These images show terrace-like features with about 0.2 μm long terraces, as presented in Fig. 1. The terrace structure could facilitate smooth 2D growth and reduce column formation during the growth of GaN epilayers other than those caused by the lattice mismatch. Following this process, the sapphire surface was chemically cleaned again to remove any contaminants acquired during the high temperature annealing process.

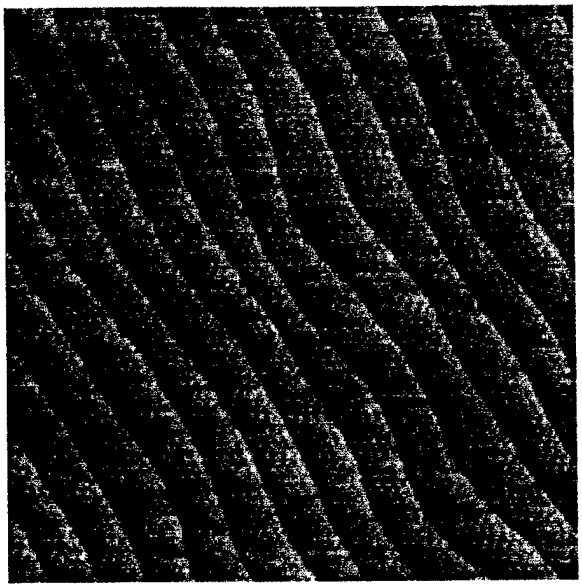

Figure 1: AFM image from the surface of a sapphire substrate before GaN growth, showing the atomic terraces. Image size is 2 x 2 μm^2. Vertical scale is 1 nm. The terrace sizes are ~0.2 μm. The step height between neighboring terraces is ~0.25 nm.

Sapphire substrates were loaded into an MBE system, which has ammonia and radio frequency activated nitrogen source for N. The substrates were heated to about 900 – 1000 °C and reflection high-energy electron diffraction system used to observe and verify a clean sapphire surface. Following this confirmation, the surface was subjected to a 5-15 min ammonia at a flow rate of 5-30 sccm for additional cleaning, reduction by H, and possible nitridation of the surface in which the sapphire surface is converted to AlN. The main nitridation process was done with the RF nitrogen source in the temperature range of 800 – 1000 °C for 10 – 30 min, with RF parameters being 300-375 W and system pressure of low

to mid 10^{-5} Torr. This was followed by growth of a 20-40 nm thick AlN buffer layer grown at temperatures of about 950 °C, higher temperatures leading to better results. The RF conditions were similar to nitridation conditions except that the nitrogen flow rate was reduced by about 20 %. The temperature of deposition however was varied between 500 and 1000 ° C. The low temperature buffer layers leading to smoother surface, but X-Ray diffraction and post GaN growth experiments indicated the high temperature buffer layers to be better in quality.

On AlN buffer layers, a 0.3 to 0.5 micron thick GaN film was grown by RF nitrogen at a substrate temperature in the range of 700 to 800 ° C while assuring, by Reflection High Energy Electron Diffraction (RHEED), smooth surface morphology. The RF power was 375 W, though values as low as 90 W was employed, and the system pressure was about 1.5 to 2. 5 x 10^{-5} Torr, depending the Ga temperature and substrate temperature employed. The goal was to obtain smooth surfaces. Higher substrate temperature required higher Ga temperatures and or lower nitrogen overpressure to get smooth and Ga terminated GaN surfaces. The growth rate employed, which was determined by nitrogen overpressure, was typically 0.4 micron per hour. On top of this GaN layer, an AlN layer of sufficient thickness to relax strain (about 5 nm or greater) at 850- 950 ° C, again making sure that the surface is smooth as determined by AFM images. Both ammonia and RF generated nitrogen source were employed, ammonia leading to sharper and more elongated RHEED patterns. Thus ammonia was adopted for this segment as the nitrogen source. The nitrogen flow condition and RF power were similar to the first buffer layer when RF activated nitrogen was used. When ammonia was used, a flow rate range of 6- 30 sccm was employed. This AlN layer was followed by a second GaN layer, similar to the previous one, and a third AlN layer. The

growth conditions for all AlN were the same and uniform growth conditions were maintained for GaN layers. This composite ends with an AlN layer on the surface. The purpose of the last AlN layer is to change the lattice constant of the template from that of GaN to that of AlN and to further growth of multiple GaN/AlN quantum dot layers. On the top of quantum dot structure either remained as it is for determination of GaN QDs properties or a GaN layer finally grown for defect reduction study by comparing with the GaN epilayer without QDs. A schematic diagram of a complete sample structure described above is shown in Fig. 2.

The typical thickness of the GaN and AlN layers in the quantum dot structure is from 1 to a few nm. Three distinctly different methods were used to create quantum dots with a reactive MBE system equipped with ammonia or RF excited nitrogen as the nitrogen source. The degree of success in the formation of quantum dots depends strongly on the surface on which they are formed. If the surface topology prior to dot formation is not atomically smooth, the topology will interfere with free formation of dots in that they may form where the topological features are as opposed to forming at or near dislocation sites. This is because of reduced strain between the dots as they grow and the underlying AlN. Even when they form, their shape can be affected by the topology. The goal is to remove topological features to facilitate dot formation on or near the defects to the extent possible. The main purpose of growing above-mentioned a few sets of AlN and GaN layers is to accomplish atomically smooth surface used as template. On top of this template, dots can be formed by various methods. The GaN layers were grown in the thickness range of 4 to 6 monolayers (about 1 to 1.5 nm in thickness) on top of QDs. This thickness range overlaps with relaxation or critical thickness. At much lower temperatures, the reported data indicate that GaN layers tend to three-dimensional growth after a short two-dimensional nature (Stranski-Krastanov growth

mode). However, the dots so formed do not exhibit high quality optical response. In this approach, a GaN layer, which must be thicker than the critical thickness, is grown and the growth is interrupted. During the interruption, the two dimensional growth is converted to three-dimensional growth. We have employed interruption periods of anywhere from 15 seconds to 2 minutes. The interruption period was followed by the deposition of AlN in the thickness of about 10 nm. This process is repeated 10 times, meaning GaN growth on AlN, interruption for 3-D formation, and AlN growth.

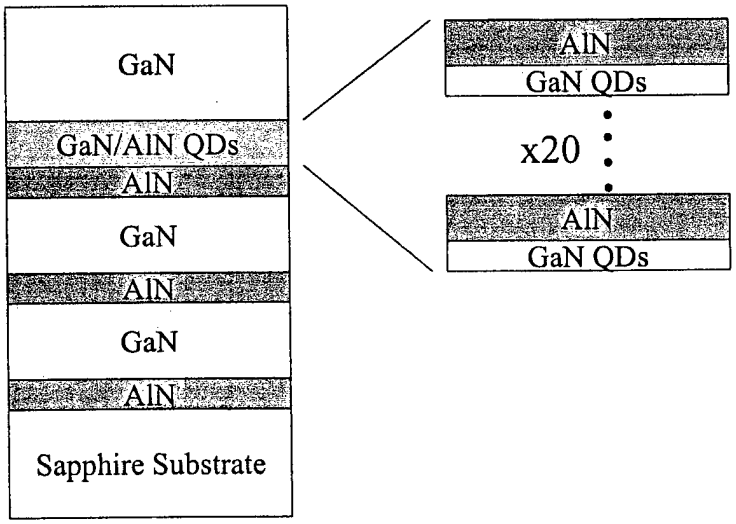

Figure 2: Schematic diagram of a typical sample structure containing a few GaN and AlN and a set of GaN/AlN quantum dot layers (from mono to multiple layer stacks).

3. Formations and Controllability of QDs Density and Size

There are mainly three method used in GaN QDs growth. In one method, GaN is grown two-dimensionally on AlN. An interruption scheme is then employed to cause the smooth GaN to morph to 3-D growth, i.e. dots. This will be called the modified Stranski-Krastanov (S-K) method. In the second method, will refer to it as the spray method, a spray of Ga atoms are directed on the template surface followed by morphing it to GaN under nitrogen flow. Though RF nitrogen can be used, ammonia was used in this case. In the third method, GaN is grown on AlN to a sufficient thickness at a particular temperature. If parameters are chosen correctly, GaN grows smoothly first followed by balling up, or three-dimensional growth. This will be called the S-K growth method. In each of these methods, each layer of quantum dot formation is followed by an AlN deposition. The pairs of GaN and AlN quantum dot layers were grown with ammonia at a flow rate of 30 sccm for the modified S-K mode, and RF for S-K mode, though other flow rates could be used, at a substrate temperature in the range of 720-935 °C. In the case of the spray method, ammonia flow was 10 sccm. Increased and decreased flow rates caused deterioration in dot formation. A temperature range of 750 to 800 was employed.

Growth temperature (T_s) is one of the key growth parameters to control the QD structures, including the geometry and density. At lower temperature, the Ga atom diffusion length is smaller, thereby, the QD density is higher. We keep the pressure constant ($1.3x10^{-5}$ torr) for all the growths, while change the growth temperature T_s. Fig. 3 shows the AFM images of S-K growth mode QD structures at three different growth temperatures. The dependences of the QD density and geometry on the growth temperature T_s are obvious. Fig. 4 shows the dependence of the dot density on the growth

temperature. At lower growth temperature, the dot density is higher, while at higher T_s, the density is lower. This dependence provides different opportunity for different application of QD structures. When the QD layer is used to reduce the dislocations, the relatively higher density of QDs is necessary to match the number of the threading dislocations, for example $10^{10}cm^{-2}$. However, when used for the electronic devices, for example single QD devices, the lower density is preferred.

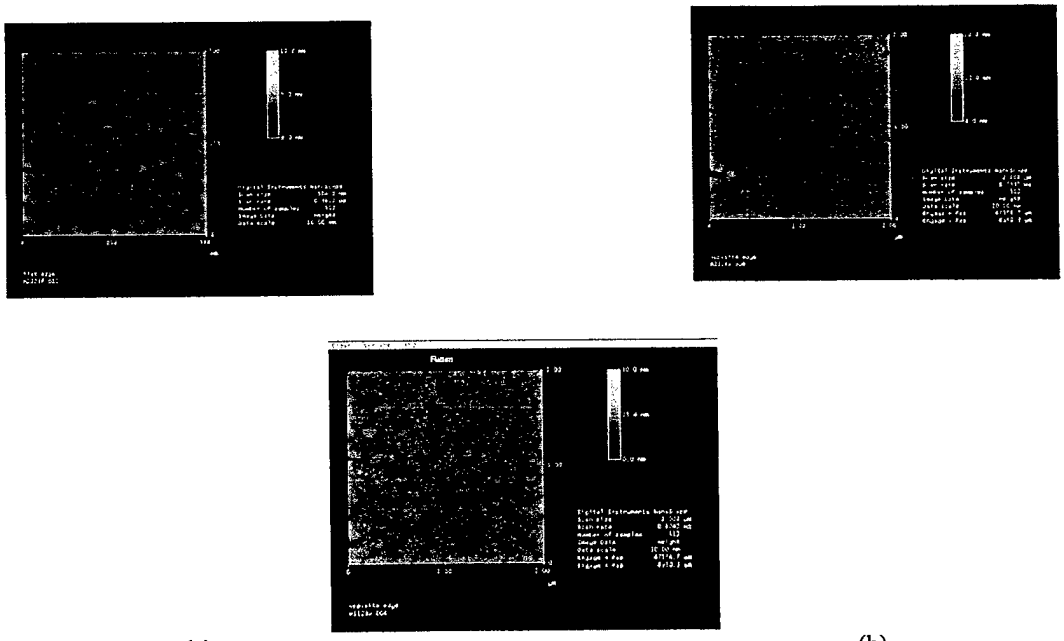

(a) (b)

©

Figure 3: AFM images of QDs grown at different growth temperatures. (a) T_s=720 °C, (b) T_s=760 °C, (c) T_s=790 °C

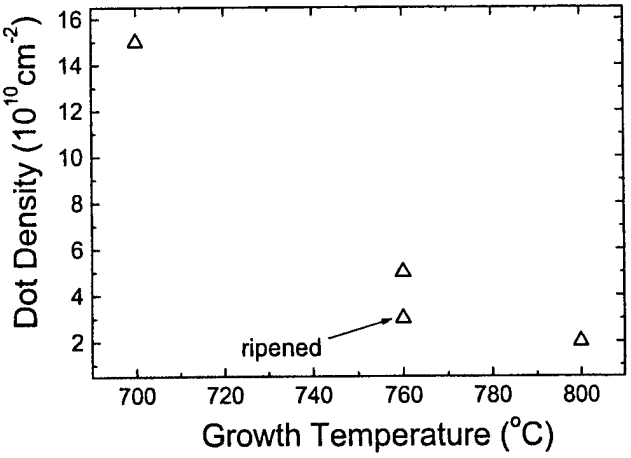

Figure 4: Growth temperature dependent QD density.

Fig. 5 shows the growth temperature-dependence of the QD height and diameter. As seen from the figures, higher growth temperatures give lower QD density, however, higher growth temperature will give larger QD diameters and larger QD heights. The QD diameter determines the lateral quantum confinement, which is a key parameter to get zero dimensional properties. For this purpose, the lower T_s is preferred.

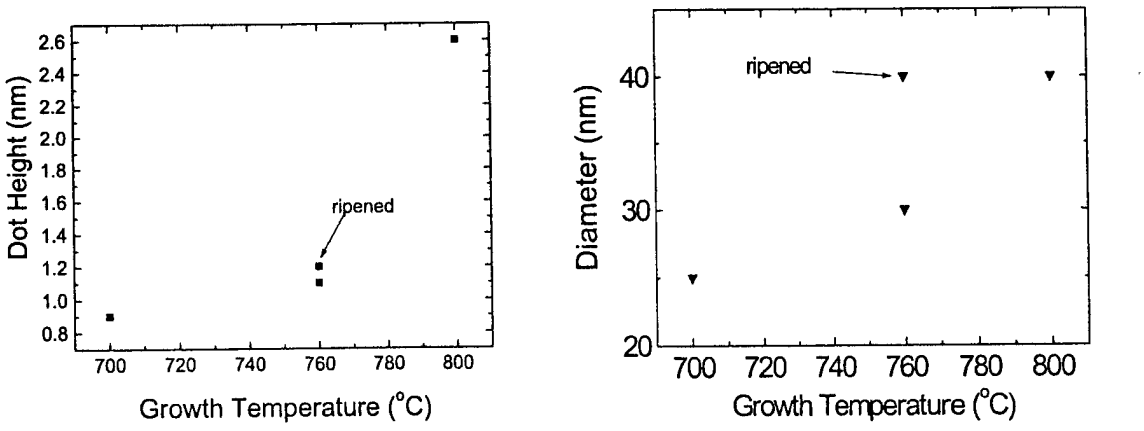

Figure 5: (a) Growth temperature Ts dependent QD height. (b) Growth temperature Ts dependent QD diameters.

To control the QD geometry, in-situ annealing (ripening) effects are useful. Fig. 6 shows AFM images of two QD samples, which are grown with the same conditions, except (b) sample is ripened under vacuum for 2 minutes. The ripening decreased the QD density, increased the dot diameters and heights, which are shown in Figures 4 and 5.

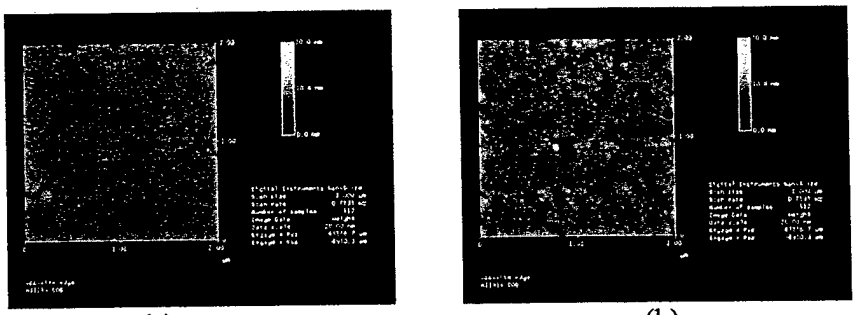

(a) (b)

Figure 6: (a) AFM images of QDs grown at 760 °C. (b) AFM images of QDs ripened under vacuum for 2 mins after grown at 760 °C.

The activated nitrogen pressure is another key factor to determine the QD density by changing the Ga diffusion length on the AlN surface, which results in the change of QD density. We fixed the growth temperature at 790 °C, and change the pressure. Figure 7 shows the AFM images of two QD structures. Sample (a) was grown with the pressure of 1.3×10^{-5} torr, and sample (b) was grown with the pressure of 2.3×10^{-5} torr.

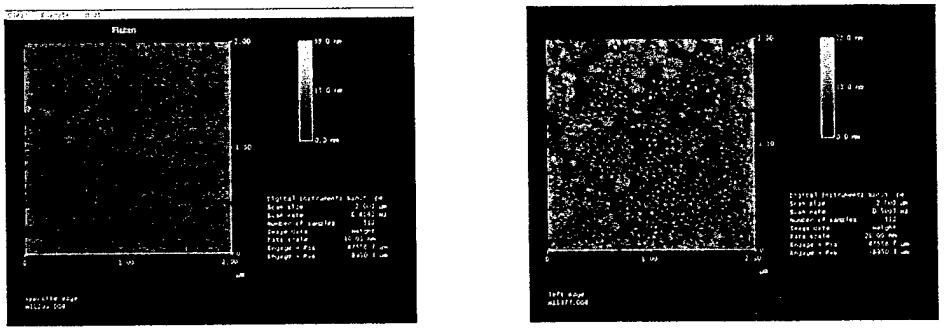

(a) (b)

(b)

Figure 7: (a) AFM images of QDs grown with the pressure of $1.3x10^{-5}$ torr (b) AFM images of QDs grown with the pressure of $2.3x10^{-5}$ torr.

The dependence of QD density and height on pressure is shown in Fig. 8. The higher pressure gives larger dot height and lower dot density.

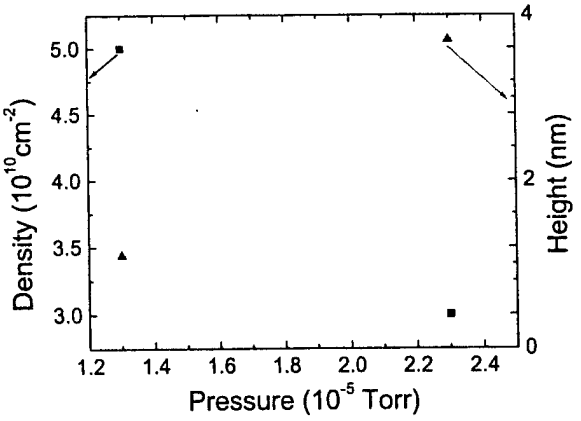

Figure 8: Pressure dependent QD density and height.

Instead of S-K mode growth of QD, there is another method to get QDs, which is called spray QD. Spray QD is formed first by spraying the Ga droplet on the AlN surface, and then use activated nitrogen or NH3 to crystallize it. The advantage of this kind of

QDs is that the wetting layer can be got rid of. We have also done some investigation of this kind of QD. FIG.7 is an AFM image of spray QD. The sample was grown at 760°C. After 14 seconds spray of Ga on the AlN surface and 15 seconds interruption, 45 second crystallization was performed with NH3 flow rate=10 sccm. QDs with 30-nm diameter were grown. The dot density is $1x10^9$ cm^{-2}

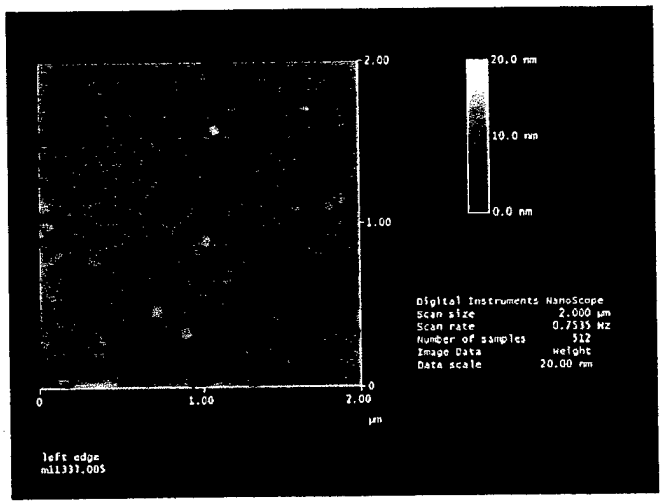

Figure 9: AFM image of spray QDs.

Another examples of AFM images of a single and 20 periods of of high density GaN quantum dot and dots as the top layers formed produced by the method employing growth interruption, modified S-K and SK method is shown in Fig. 10(a) and (b), respectively.

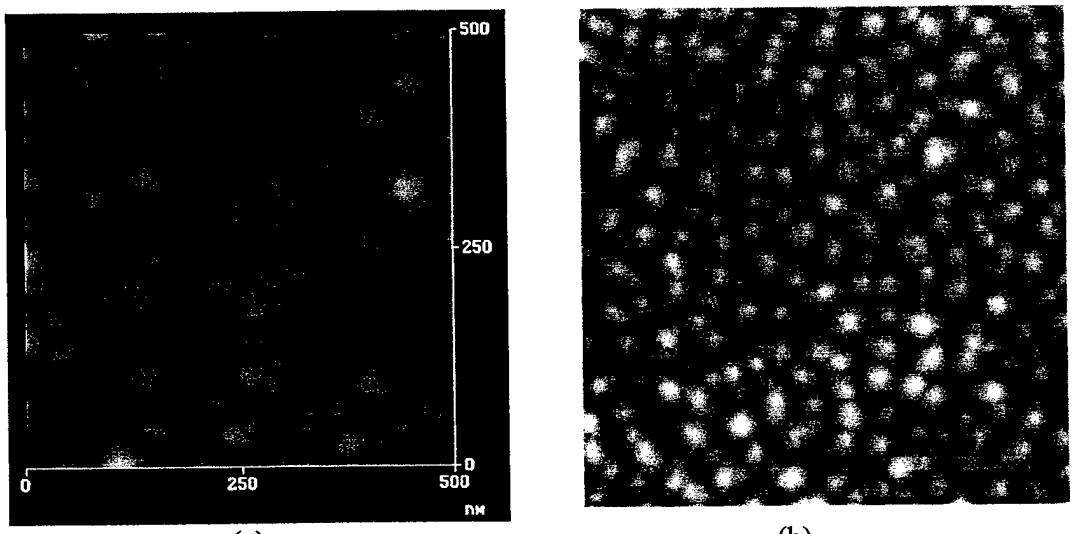

(a) (b)

Figure 10: (a) AFM image of a single layer of high density GaN quantum dots produced by the method employing growth interruption, modified S-K mode and **(b)** AFM image from the as-grown surface of a sample (SVT736) with 20 periods of quantum dots. The image size is 1x1 μm^2 and the vertical scale 20 nm. The dots were formed by the SK method.

4. Materials Characterization

Successful fabrication of GaN-based devices depends on the ability to grow high quality epitaxial films and to reliably characterize the materials. Mostly, the characterization of dislocations is carried out using TEM, a process that requires extensive sample preparation. The availability of reliable and quick methods to determine the defect density is of great importance in order to understand the correlation between growth conditions and consequently to achieve high-quality GaN layers. Wet chemical etching is a convenient technique to determine the density of defects propagating to the surface. Hot H_3PO_4, mixed H_3PO_4/H_2SO_4 solution, and molten KOH have been found to etch pits at the surface defect sites. However the origin of etch pits is still controversial and sometimes the obtained etch pit densities (EPD) is lower than the dislocation density (DD) found by TEM. Recently, it has

been demonstrated photo-electrochemical (PEC) etching for DD estimation in n-type GaN films. They reported nanometer-scale whiskers obtained by selectively etching GaN between dislocation sites and, with TEM analysis, demonstrated the whisker density to be very close to the effective DD. We have investigated defects in GaN films by PEC method and wet etching using both H_3PO_4 and molten KOH. Our purpose is to determine whether, and under what conditions these techniques are consistent in order to get to a better estimation of the defect density. We have used PEC and hot wet etching using H_3PO_4 and molten KOH to estimate the defect density in GaN films grown by HVPE and MBE. Free-standing whiskers and hexagonal etch pits are formed by PEC and wet etching respectively. Using AFM, we found the whisker density to be similar to the EPDs for samples etched under precise conditions. Additionally TEM observations confirmed DDs obtained by etching, which increased our confidence in the consistency of methods used. Because the etching procedures are simpler and less time consuming, they can be an excellent precursor to TEM analysis for determination of the DD.

Two different sets of GaN samples were used for the experiments. The first set was Si-doped ($n \sim 2 \times 10^{18}$ cm^{-3}) ~ 9μm thick Ga-polar GaN layers grown by HVPE on sapphire. The second set consisted of unintentionally n-doped GaN layers grown by MBE on sapphire. Nitridation was performed at high (890-985 °C) and low (~ 500 °C) temperatures by radio frequency (RF) N plasma, which has no apparent effect on the results. Some samples utilized GaN buffer layers grown at 500 °C, and 800 °C. Others utilized AlN buffer layers grown near 500 °C and 890-930 °C. Following the buffer layers, ~1μm thick GaN layers were grown at a temperature between 720 and 850 °C with growth rates in the range 0.3-1 μm/h under N-limited (Ga-rich) conditions.

PEC etching was carried out in a standard electrochemical cell at room temperature using an unstirred 0.02 M KOH solution and a He-Cd laser for UV illumination. A Ti mask, resistant to the etchant, was patterned around the periphery of the sample with a lift-off process. The Ti contact served to assist the photocurrent conduction. No additional bias was applied between the sample and the cathode. The morphology of GaN samples, etched by PEC and hot wet etching, was investigated using AFM and scanning electron microscopy (SEM). Additionally, some samples were observed by TEM to estimate the DD.

Slightly carrier-limited conditions with moderate illumination intensity were used to etch crystalline GaN material selectively, leaving vertical wires on the surface. The AFM image of Fig. 11(a) reveals the PEC etched surface morphology of the HVPE-grown sample. We estimated the height of whiskers to be ~700 nm and the lateral size ~100 nm. The density is about 1-2x10^9 cm^{-2}. The etched surface morphology was also investigated by SEM, Fig. 11(b). The calculated density of features (white dots) is ~ 2x10^9 cm^{-2}, the same value obtained from AFM.

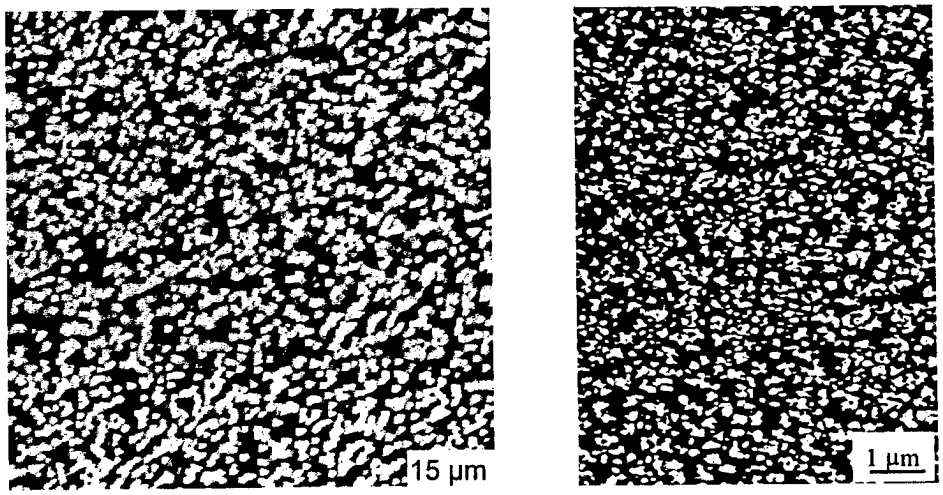

Figure 11: (a) AFM image of HVPE-grown GaN sample etched by PEC process. Whisker-like features are formed by etching with a density of $\approx 2x10^9$ cm^{-2}. The vertical scale ranges from 0 to 1200 nm. (b) Plan-view SEM image of the PEC etched sample. The density of whiskers (white dots) is ~1-$2x10^9$ cm^{-2} the same value obtained from AFM.

In order to clarify the relation between EPD and DD and look for any consistency among the various etches, we used H_3PO_4 and molten KOH as defect etchants in GaN. The AFM image of the HVPE-grown sample etched by molten KOH for 2 minutes at 210 °C is shown in Fig. 12(a). The pits, with density of $\approx 1x10^9$ cm^{-2}, are of hexagonal shape and their size ranges from 40 to 100 nm in diameter and from 10 to 30 nm in depth. Fig. 12(b) shows the surface morphology after etching in H_3PO_4 for 6 minutes at 160 °C. The EPD is the same found for the KOH etched sample and close to the density of features formed by PEC etching. During the wet etching, a careful balance must be struck to ensure that every defect is delineated, but not over-etched to cause merging which would lead to an underestimation

of the defect density. We show in Fig. 12(c) an AFM scan of the same sample etched for 10 min at 200 °C in H_3PO_4. We estimated the EPD ≈ $1x10^8$ cm^{-2}, an order of magnitude less than the correct value obtained earlier due to over-etching.

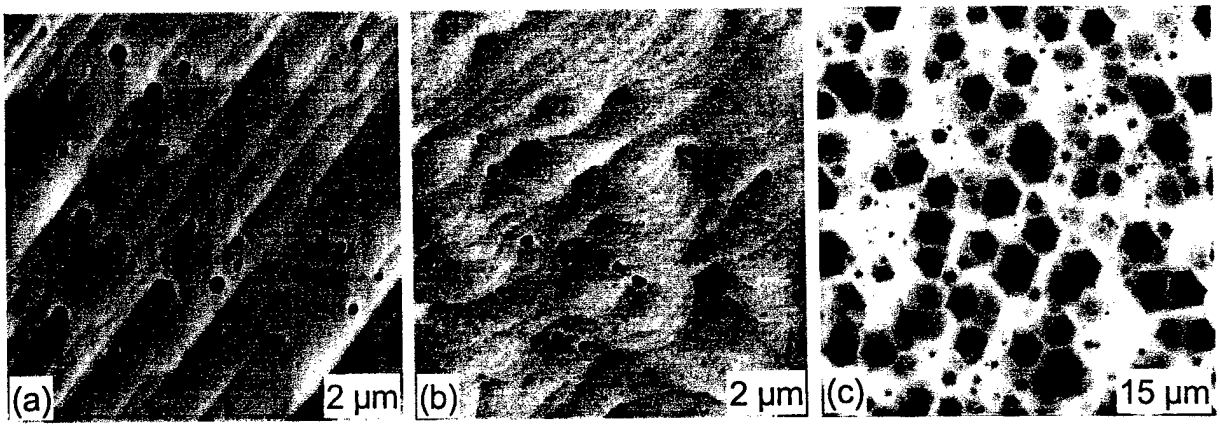

Figure 12: AFM images of the HVPE-grown GaN surface morphologies produced by wet etching. (a) Surface morphology after etching in molten KOH for 2 min. at 210 °C. Pits at the defect sites are formed with a density of $1x10^9$ cm^{-2}. (b) Surface morphology after etching in H_3PO_4 for 6 min. at 160 °C. The EPD is the same found for the KOH etched sample. The vertical scale ranges from 0 to 10 nm. (c) Surface morphology after etching in H_3PO_4 for 10 min. at 200 °C (EPD ≈ $1x10^8$ cm^{-2}). The vertical scale ranges from 0 to 450 nm.

We characterized the HVPE-grown sample using TEM in order to get the effective DD and compare this value with the defect densities found by defect revealing wet etches. TDs, primarily of edge or mixed character, were observed starting from the buffer/GaN interface and often stopping within the 9 μm-thick layer. Hexagonal nanopipes are also seen with sizes in the range 4-10 nm and density ≈ 5-$10x10^7$ cm^{-2}. In all the defect density, close to the top surface, was estimated ≈ 0.5-$2x10^9$ cm^{-2}, similar to the values obtained by defect revealing etches. The defect delineation etch was also tested on the GaN films grown on

sapphire substrates by MBE, and the results were compared to those from TEM. Fig. 13(a) shows the AFM image from the etched surface of a MBE grown GaN film (SVT381). The TEM image from the same sample is shown in Fig. 13(b). As demonstrated, the density of the pits resulted from defect delineated etch is very good agreement with the dislocation density observed in the TEM image. The results of these investigations establish the validity of the etching process for defect delineation. There is no doubt that the defect delineation etch is sensitive to structural defects and that when done properly, which was done in this case, the absolute values are dependable. In addition, when this process is employed in a series of layers, which parametric changes, the relative values and trends that are established are very important and lend additional credence to the technique.

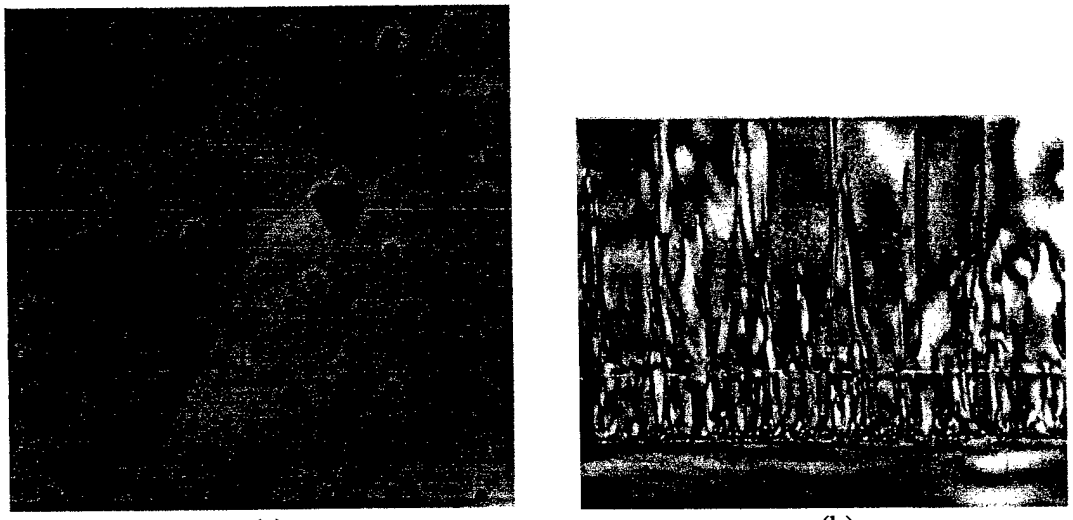

(a) (b)

Figure 12: (a) AFM image (5x5 μm^2) from the MBE grown Ga-polar GaN surface after etching in H_3PO_4 for 5 min. at 160 °C. Hexagonal pits are formed with a density of $\approx 1x10^9$ cm^{-2}. The vertical scale ranges from 0 to 10 nm. (b) Cross-sectional TEM image of a Ga-polar GaN layer. The total DD, near the top surface, is about $3x10^9$ cm^{-2} (edge dislocations about 95 % of the total).

5. Dislocation Reduction Using Quantum Dot Buffer

We have investigated a new method of improving GaN crystal quality by utilizing a stack of quantum dots (QDs) in GaN grown on sapphire substrates by molecular beam epitaxy. The GaN films were grown on GaN/AlN buffer layers containing multiple QDs, as shown in Figure 2, and were characterized by x-ray diffraction, photoluminescence, atomic force microscopy, and transmission electron microscopy. The density of the dislocations in the films was determined by defect delineation wet chemical etching and atomic force microscopy. It was found that the insertion of a set of multiple GaN QD layers in the buffer layer effectively reduced the density of the dislocations in the epitaxial layers. As compared to high density of dislocations ($\sim 10^{10} cm^{-2}$) in typical GaN films grown on AlN buffer layer, a much lower density of dislocations was demonstrated in the GaN films grown with quantum dot layers. Transmission electron microscopy observations showed disruption of the threading dislocations by the QD layers.

Three sets of samples investigated were grown on c-plane sapphire substrates by MBE with both ammonia and radio frequency activated nitrogen sources. The growth sequence of the first set samples include an AlN layer (~10nm) on substrate, a GaN layer (~ 300nm), a second AlN layer (~10nm), a second GaN layer (~200nm), and a third AlN layer (~10nm). All three AlN layers were grown at high temperature of ~950°C. Although the low temperature AlN may lead to a smoother surface, but X-ray diffraction (XRD) and post GaN growth experiments indicated that the high temperature buffer layers give better crystal quality. The GaN layers were grown at ~800°C. The growth rate of GaN was ~ 0.4 μm/hour.

In addition to the above structure, a 20 period GaN/AlN QDs were further grown for the second and third set samples. The growth temperature for the GaN/AlN QDs was

~800°C. The GaN layers were about 4 atomic monolayers thick (~1 nm in thickness). The AlN spacer layers were in the thickness of ~2 nm. For the second set samples, the growth was stopped when the growth of 20 periods GaN/AlN QDs was completed. For the third set samples, an additional GaN layer (from ~ 0.1 to 1.6 μm) was grown at a temperature 740°C-950 °C on the top of QDs.

The density of dislocations near the surface of the epilayers was examined by the wet chemical etch and AFM measurements. Hot (160°C) phosphoric acid (H_3PO_4) was used as the chemical etchant. The resulting pits, mostly of hexagonal shape, appear after the surface was etched. An AFM image of the as-grown and the etched surfaces of a sample from first set (sample A) is shown in Fig. 13(a) and Fig. 13(b), respectively. The size of both images is 1x1 μm^2. The vertical scale is 30 nm for image *a* and 20 nm for *b*. The etching time for the image b is 15 seconds. As in a typical Ga-polar GaN film grown by MBE, the hot wet chemical etching results in hexagonal pits at the defect sites on the surface. Due to the high density of defects, many etched pits are already mixed together even with a short etching time. A very rough estimate of the pit density by counting the number of the etched pits is on the order of 10^{10} cm^{-2} or higher. This value is, however, typical of GaN films having thicknesses ~1 μm grown by MBE on sapphire substrates using AlN as the buffer layers

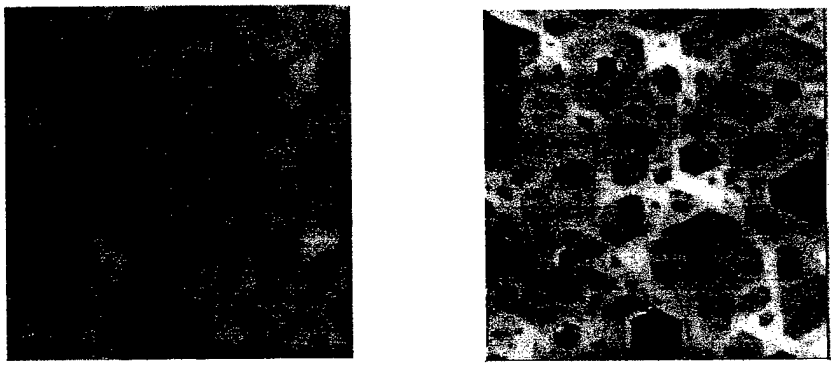

(a) (b)

Figure 13: AFM images from (a) the as-grown and (b) the etched surface of sample A grown on a GaN/AlN buffer which does not include any quantum dot layers. The image sizes for both images are 1x1 μm^2. The vertical scale is 30 and 20 nm for (a) and (b) respectively. The etching time for (b) is 15 seconds.

AFM images of the as-grown and etched surfaces of a sample from third set (sample C) are shown in Fig. 14(a) and Fig. 14(b), respectively. The size is 1x1 μm^2 for image a but is 10x10 μm^2 for b, in order to show the density of the etched pits. The vertical scale is 10 and 50 nm for images *a* and *b* respectively. Etching time for image b is 12 minutes. All etched pits have hexagonal shapes and their sizes are relatively uniform with diameters of ~500 nm. The enlarged scan from the etched surface does not show additional pits. Well separated etch pits on the etched surface allow us to reliably count the pit density, which is ~$5x10^7$ cm^{-2}. Thus, in comparison to sample A, a reduction in the density of etched pits by more than two orders of magnitude is evident in sample C.

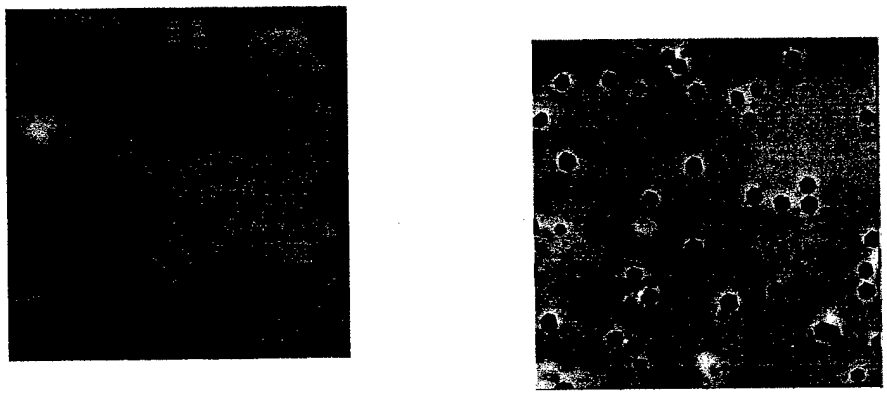

(a) (b)

Figure 14: AFM images from (a) the as-grown and (b) the etched surface of sample C grown on a GaN/AlN buffer including an additional multiple quantum dot layer. The image size is 1x1 μm^2 and 10x10 μm^2 respectively. The vertical scale is 10 and 50 nm for images (a) and (b), respectively. Etching time for image (b) is 12 minutes. The diameter of the hexagonal pits observed in image (b) is approximately 500 nm.

To demonstrate that the density of the etched pits is independent of etching conditions, the surface morphology of a sample subjected to different etching times was also examined. Fig. 15(a) and Fig. 15(b) show the etched surface of the sample C with 6 and 10 minutes etching respectively. The sizes of both images are 2x2 μm^2. The vertical scale for both images is 30 nm. As Figure 10 and Figure 9b show, the density of the etched pits does not change with etching time. Only the size of the pits changes. When the etching time increases from 6 to 10, and to 12 minutes, the pit size increases from ~200 to ~400, and to ~500 nm as shown in Figure 10a, 10b, and 9b, respectively.

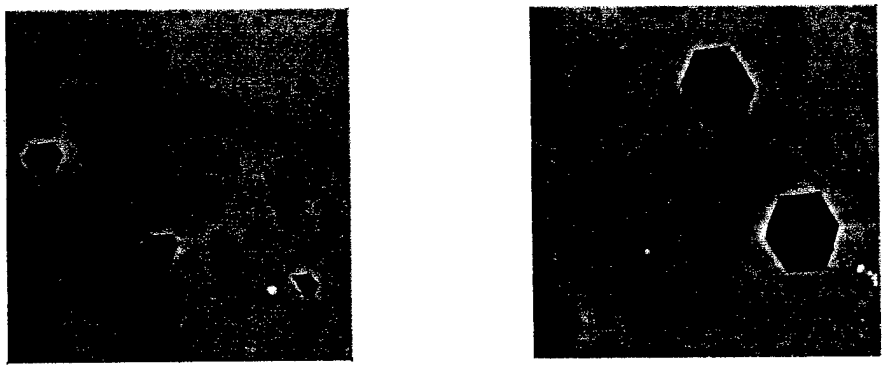

Figure 15: AFM images from the etched surfaces of sample C grown on a GaN/AlN buffer including an additional multiple quantum dot layers. The etching time is 6 minutes for (a) and 10 minutes for (b). The sizes of both images are 2x2 μm^2. The vertical scale for both images is 30 nm. Diameters of the three pits observed in image (a) are ~200 nm or less. Diameters of the two pits observed in image (b) are near 400 nm.

The microstructure of the crystal near GaN/AlN QDs and underneath GaN layer was studied in cross-sectional geometry using TEM. Fig. 16(a) is a low-magnification TEM image from a sample from second set (sample B) showing the entire epilayer up to the GaN/AlN QD multilayers. Darker contrast corresponding to threading defects is visible extending through the middle AlN thin layer, and up to the bottom of the QD region. Almost without exception, these defects do not appear to continue any further into the GaN/AlN QD epilayer. Fig. 16(b) is a higher magnification image mostly showing the GaN/AlN multilayer. Threading defects are again visible that terminate at the top of the thick GaN layer or the thin AlN buffer layer. Fig. 17 shows a cross-sectional image of a sample, which includes the final GaN capping layer. Some threading defects are visible in the uppermost GaN layer but their positions do not appear to be related to those present in the underlying GaN layer.

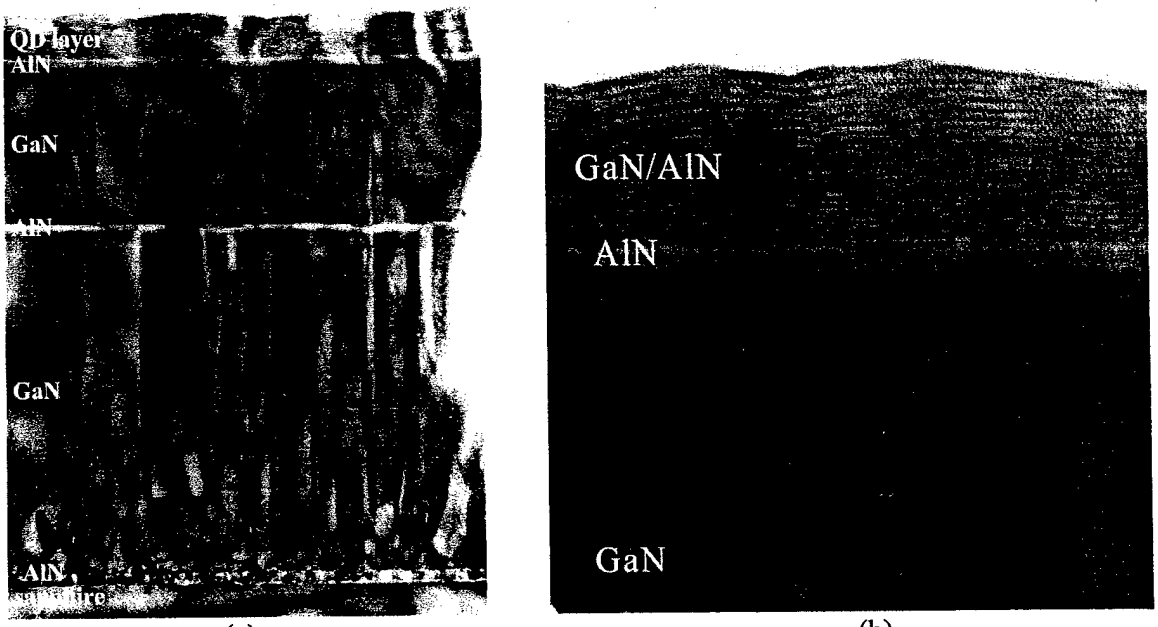

(a) (b)

Figure 16: (a) Cross-sectional TEM image of a sample with top GaN/AlN quantum dot layers. (b) Cross-sectional TEM image showing top of the sample.

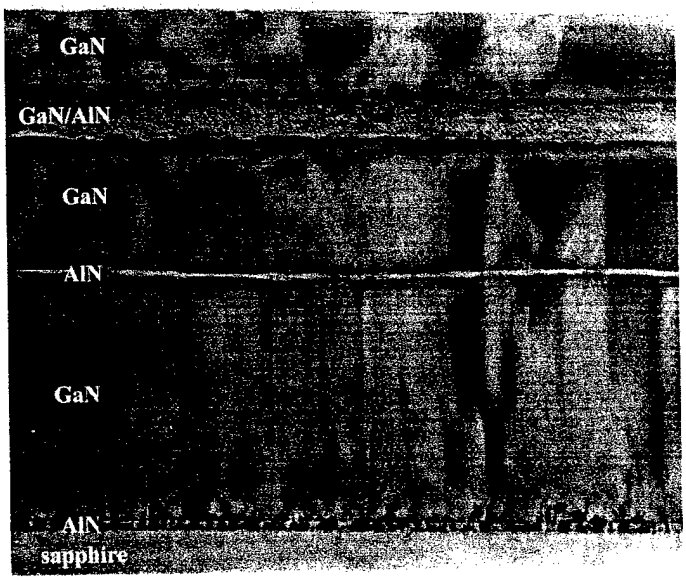

Figure 17: Cross-sectional TEM from a sample with top GaN layer.

We also characterised the samples with PL and XRD measurements. Fig. 18(a) and Fig. 18(b) show the room temperature PL spectra from samples A and C respectively. The excitation source is the 325.0 nm line from a He-Cd laser. For sample A, the PL spectrum shows two bands. The one at 3.4 eV is from band edge with a full width at half maximum (FWHM) of ~0.1 eV. The yellow band at ~2.3 eV is broader and it is defect-related. The weak band edge PL and the pronounced yellow band are typical for thin Ga-polar GaN films grown on sapphire substrates by MBE using simple AlN buffer layers. The PL spectrum from sample C is very different. The band-edge PL near 3.4 eV is more than 10 times stronger and the yellow band is weaker than the spectrum from sample A. In addition, the band-edge PL is broader (FWHM of ~0.15 eV) and may contain a couple of separate peaks. This PL band is mainly from QDs. The high PL intensity is essentially due to the confinement (or localisation) of the photo-carriers in QDs, and to the reduced carrier scattering by bulk or surface defects. The broadening of this PL band originates mainly from size fluctuations of different QDs. In the case of small dots, the effect of confinement and strain leads to a blue peak-shift with respect to the GaN band gap, which gives the high energy component in the PL band. In the case of large dots, the effect of polarisation may lead to a red peak shift, which gives the low energy component.

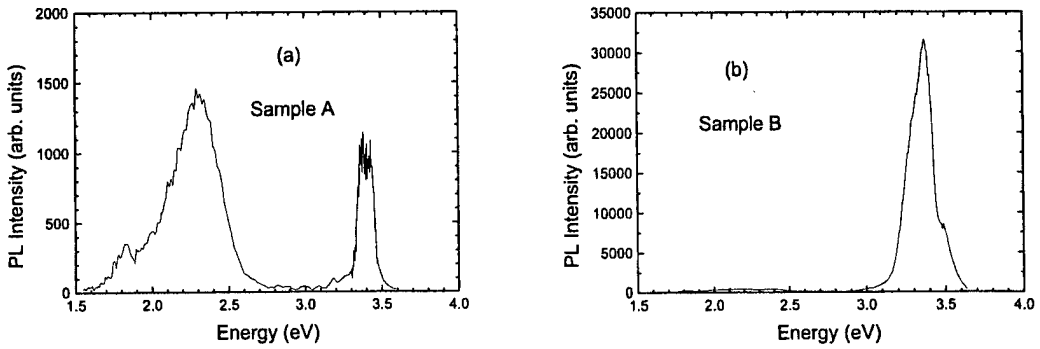

Figure 18: PL spectra from sample A (a) and sample C (b) measured at room temperature. Note the different intensity scales of the two spectra.

In comparison with the GaN films grown without QDs in the buffer layer, the samples with QDs generally showed narrower XRD peaks, typically from 1 to 2 arc-minute for the [002] peak. The asymmetric (104) peaks were broader (~7 arc-minutes).

We believe that the significant reduction in the dislocation density revealed by the etch pits and by the TEM images in the samples set C, is essentially due to the introduction of the multiple QDs layers. In the case of lateral growth on the SiO_2 patterned GaN surface, it was found that the dislocations from the GaN were blocked by the SiO_2 and the lateral growth on the SiO_2 shows a very low dislocation density. In our case, the dislocations extending from the film/substrate interface in the sample sets B and C may also be interrupted by GaN QDs. For example, the dislocation lines that have an in-plane component may loop around the QDs and no longer extend into the sample surface. Dislocations may also terminate at the surface of the dots. The partially lateral growth of the GaN QDs and the AlN spacer layer may also have contribution to the observed low dislocation density.

6. Investigation of GaN/AlGaN MQW back-illuminated Schottky barrier UV photodetectors

III-V nitride based devices are an ideal candidate for UV detection in a number of applications including early missile plume detection, flame sensing, UV astronomy, space-to-space communication and biological effects. In the past decade, there have been several reports on GaN-AlGaN based photoconductors, p-n junction, p-i-n and p-π-n, Schottky barrier, Metal-Semiconductor-Metal, Metal-Insulator-Semiconductor, Field-Effect Transistor or Bipolar Junction Transistor, and avalanche photodiode.

To date, most of the work on III-nitride UV photodetectors, inclusive of all types, has relied on bulk-like epilayers. However, for other III-V material systems, such as GaAs or InP based, devices containing single or multi-quantum wells in their active region have been successfully grown, fabricated and demonstrated. In a 2D system, a high joint density of states enhances the oscillator strength, due to confinement, for upward carrier transition and gives rise to enhanced optical absorption, and hence a higher quantum efficiency in photodetectors. Strong piezoelectric fields, such as those that exist in GaN quantum wells would also improve the carrier transport. Recently, GaN/AlGaN MQW UV photodetectors have been fabricated in a planar geometry and reported with 0.03A/W peak responsivity. The aim of the current work is to present the primarily experimental results on back illuminated vertical Schottky type MQWs UV detectors and describe carrier transport congruent with experimental results of successively designed three structures.

Three detectors referred as svt1171, svt1172, and svt1174 were designed, grown fabricated, and characterized. They were grown by molecular beam epitaxy using an rf-

plasma nitrogen source. Figure 19 shows the schematic of the device structure and potential profile.

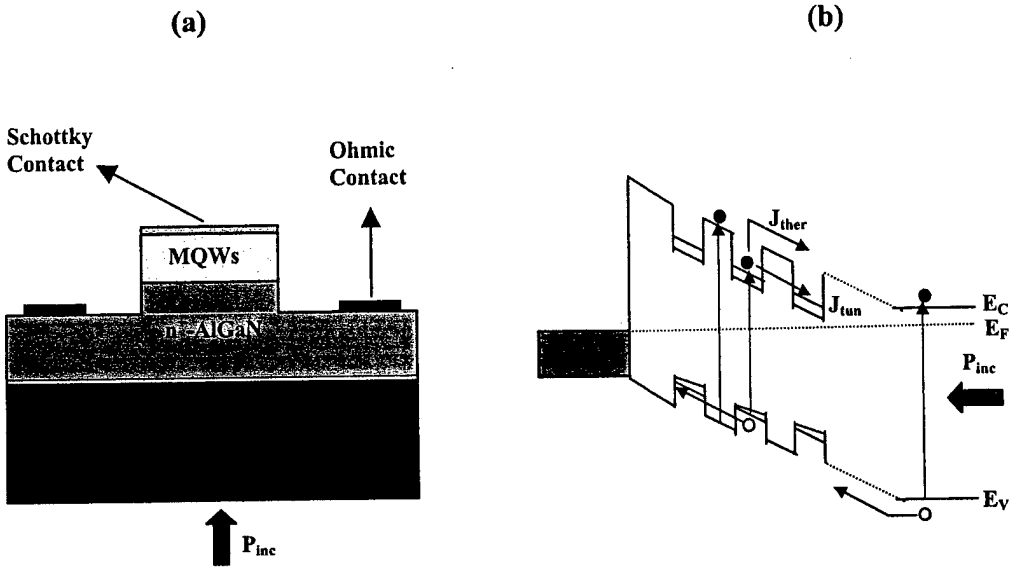

Figure 19: (a) Schematic structure of a back-illuminated Schottky barrier multi-quantum well UV photodetector. Growth parameters are given in the text, and **(b)** Schematic conduction and valance band profiles of MQW Schottky device together with carrier transport.

The growth was initiated by a thin layer of AlN buffer layer (~50 nm) on top of a *c*-plane sapphire substrate following routine thermal annealing and nitridation. Then, a Si-doped AlGaN layer of ~0.35μm with a 0.27 AlN content was grown as the short wavelength cutoff region on top of the AlN buffer layer. The active layer for all the three-detector structures consisted of a 20 periods of GaN/AlGaN MQWs with 3nm well thickness. The thicknesses of barriers were varied as 7nm, 5nm and 3 nm for svt1171,

svt1172 and svt1174, respectively. The growth sequence was finished by growing a thin AlGaN cap layer. All the grown layers were performed under Ga-rich conditions, inclusive of the AlGaN layers, which is novel. Fabrication of vertical geometry Schottky diodes was initiated with the definition of mesas using reactive ion etching (RIE) in BCl_3 plasma. The bottom ohmic contact was made by e-beam and thermal evaporation of Ti/Al/Ti/Au. Rapid thermal annealing for 1 min at 900 °C was used to yield good ohmic behavior. A Ni/Au layer composite was used for the Schottky contact as a circular pattern on front side of the wafer, with an area being $0.03mm^2$.

The spectral responsivity for each detector was measured with the aid a UV-enhanced Xe arc lamp and the wavelengths contained therein were dispersed by a monochromator. The light source was calibrated against a calibrated UV-enhanced Si photodetector. The dispersed light was modulated with a mechanical chopper and focused on the backside of the device. The signal was amplified and analyzed by a standard lock-in technique.

Figure 20 shows the absolute spectral response of the investigated detectors without bias. The responsivity is nearly flat between 350nm and 325nm for svt1174 and slightly blue-shifted for svt1172 and svt1171. The long wavelength cutoff wavelengths are at 357 for all three devices, which are attributed to ground state electron-heavy hole absorption in the MQW. The polarization-induced electric fields result in a red shift of the long wavelength cutoff. From room temperature PL measurements we found the peak wavelengths of GaN/AlGaN MQW excitonic emissions at 387nm, 377nm and 367nm for svt1171, svt1172 and svt1176, respectively. The difference between emission and absorption edge is due to the defect induced Stokes shift. They confirm that absorption of

photons by MQWs determines the long wavelength cutoff. Therefore, one can change the long wavelength absorption edge of the MQWs detectors by adjusting well width and Al composition. An n-type AlGaN absorption layer below the MQWs causes the short wavelength cutoff at 301nm, 305nm and 312nm for svt1171, svt1172 and svt1174, respectively. The Al contents in this absorption layer are between ~0.25-0.3, which are also confirmed by XRD, reflectance and transmittance measurements. Single-side polished back-illuminated MQWs detectors exhibited a peak responsivity value as high as 0.054 A/W for svt1174, corresponding to 20% quantum efficiency. The particular sample has a thinner barrier thickness among the others. The inset of Figure 20 shows the transmittance ratio between single-side and double side polished sapphire. As seen from the inset, the double side polished sapphire transmits the light more than 2.3 times compared to single-side sapphire in the spectral region where devices show flat responsivity. Therefore, we would expect a peak responsivity value as high as 0.12 A/W for svt1174 had the backside been polished. For the other detectors, svt1171 and 1172, the expected peak responsivities are about 0.035 A/W and 0.074 A/W, respectively. Although device structures are identical, with the exception of the barrier thickness of quantum wells, they gave markedly varying peak responsivity values, which will be elaborated on later in the context of a phenomenological model.

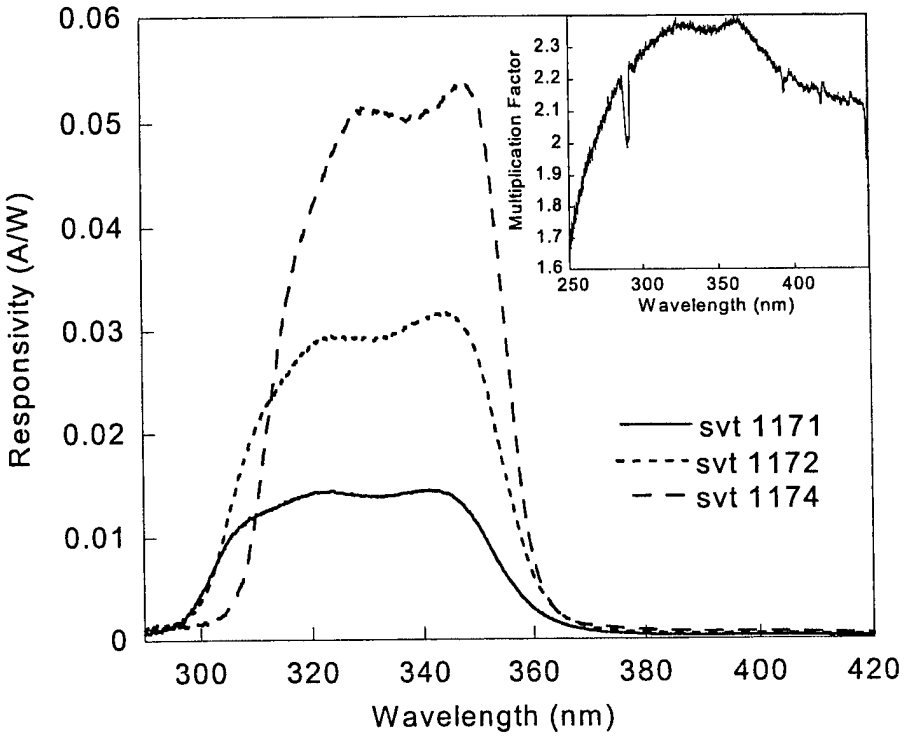

Figure 20: Comparison of the unbiased spectral responsivity for all three MQW photodetectors. Inset: The transmission ratio between the single and double-side polished sapphire.

The dependence of the responsivity on the incident power density was determined by using a non-focused 325nm He-Cd laser. The optical power intensity was varied by using calibrated neutral density filters. The photocurrent exhibited a nearly linear increase with incident optical power up to $1kW/m^2$ for all three devices, as shown in Fig. 21.

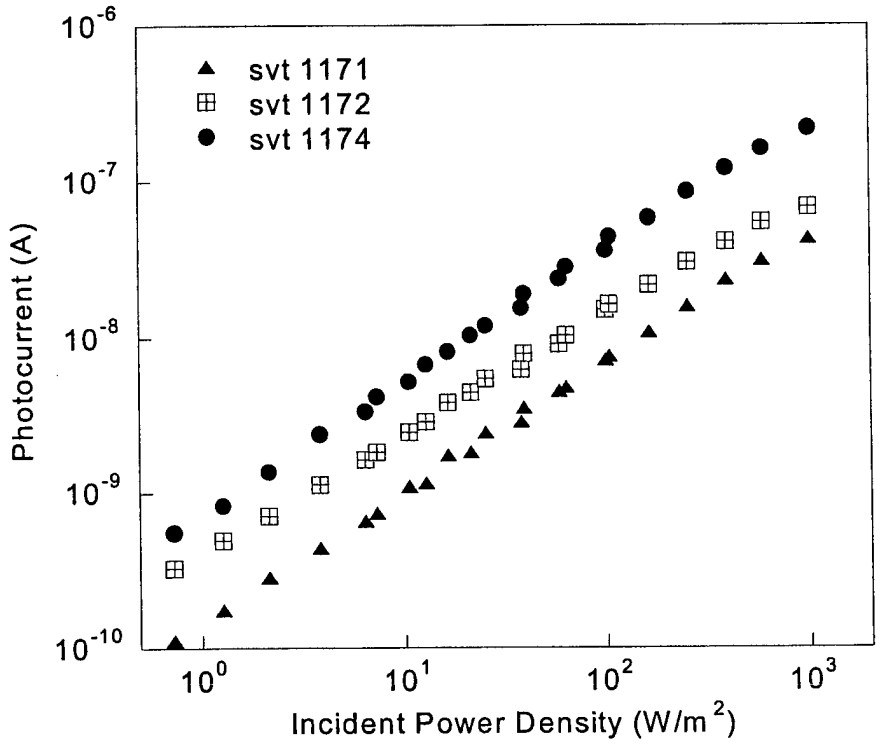

Figure 21: Linear Photocurrent dependence on the optical power density, measured with a He-Cd laser (325nm).

We have also studied bias dependence of the responsivity for all three types of detectors up to –5 V. Since the devices made using svt1171 and svt1172 display similar bias characteristic, only the results from svt1174 will be presented here as an example to avoid repetition. Figure 22 shows the spectral responsivity taken at different bias voltages for svt1174. As seen from the figure, the spectral responsivity curve does not show any significant difference as far as the shape is concerned, but the noise level increases with applied bias because of the voltage source. The inset in Figure 22 shows the peak

responsivity at 350nm as a function of applied bias. Below –2 V, the responsivity increases linearly with applied voltage. Above –2V the responsivity saturates at 0.19 A/W. The saturated responsivity values for svt1171 and svt1172 were obtained as 0.052 A/W and 0.12A/W, respectively. The ratio between the saturated peak responsivity and zero bias peak responsivity is about 3.6 times and the same for all devices, supporting the effect of the barrier width, which is discussed next.

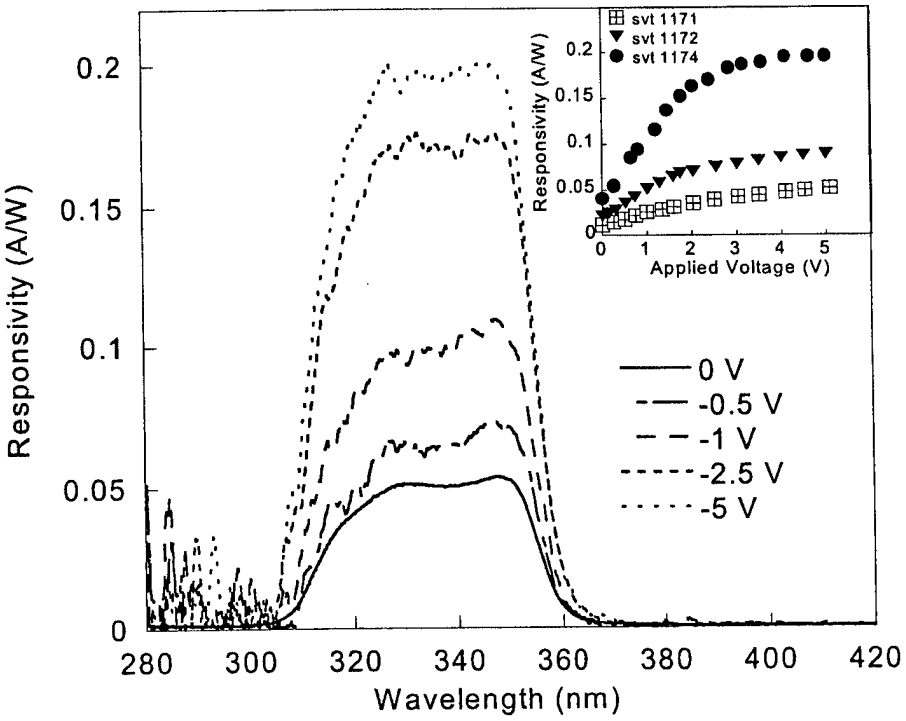

Figure 22: Spectral responsivity at different bias voltages for the device fabricated using svt1174. Inset: The peak responsivity vs. the applied voltage for all three devices.

The operation mechanism of MQW photodetectors under investigation can be understood in the context of the potential profile. Fig 1(b) shows the schematic potential profile for carrier transport involved in the device operation. As can be seen from the figure, in contrast to photodetectors using bulk GaN or AlGaN layers, the GaN/AlGaN MQWs are placed in the depletion region of the Schottky barrier junction. When the light is incident on the device, electron-hole pairs are created by absorbing photons whose energy is greater than the ground state e-hh energy difference. This absorption edge basically determines the long wavelength cutoff of the detector as observed in the spectral responsivity measurements, and is also verified by room temperature PL absorption spectra demonstrating a very small Stokes shift. The created electron-hole pairs are swept away by means of thermionic and tunneling processes, which are also shown in the figure. Note that the tunneling current can also be accompanied by emission or absorption of phonon and defect/trap related processes.

In order to gain an insight whether our model is applicable, we designed three similar MQWs detectors by changing only the barrier thickness of the quantum well structure, following otherwise identical growth and fabrication procedures. As is clearly seen in Figure 20, when the barrier thickness decreases, the peak responsivity increases due to the increase in the transmission probability of carriers and hence the tunneling current. An improvement of a factor of four times in the peak responsivity was achieved using the thinnest (svt1174) compared to the thickest (svt1171) barrier structure. Possibly, further design consideration may enhance the detector performance.

By analyzing bias dependence of the responsivity in detail within the context of the model we can gain insight and optimize the device structure more efficiently. As is

seen from the bias measurements (Fig. 22), the peak responsivity increases with increasing applied reverse voltage due to the increased electric field across the increased depletion region. Thus, a combination of increased band bending and the depletion region encompassing more of the quantum wells enables a more efficient carrier collection at the terminals, leading to a higher current across the external circuit. It should be noted that the field in the depletion region is a combination of polarization-induced field and that induced by applied bias. At higher applied bias voltages, the measured responsivity exhibited photoconductive gain probably originating from defects at the surface and/or within the depletion layer. Then, it tends to saturate due to sweep-out effect. When we compare the ratio of the zero bias and the saturated peak responsivity of all three devices, almost a constant value is found. This shows, even if we take into account a 40nm extra layer thickness between the sequential device structures (svt1171, svt1172, and svt1174) in the depletion region, that the current even at higher bias voltages is limited by the carrier tunneling probability which increases for smaller barrier thickness. All these experimental evidence supports our phenomenological model involved in the current mechanism in the investigated MQW Schottky type UV photodetectors.

7. Summary

In summary, in the first par of the report, we mainly investigated the controllability of the GaN/AlN quantum dot (QD) growth using the S-K growth mode. The controllability of QD density and size was investigated by changing the growth temperature, III/V ratio etc. AFM images give direct information of the QD structures. QDs grown with spray of Ga droplet and then crystallization is also investigated.

In the second part of the report we have used PEC and hot wet etching to estimate the defect density in GaN films. In the case of PEC, free-standing whiskers in defect sites are formed after etching. In the case of wet etching, the acid attacks only defect sites in Ga-polar films producing nanometer-scale pits but leaving the defect-free GaN intact. Using AFM, both whisker and pit densities were determined and the similar results were observed. TEM study confirmed DD obtained by etching which increased our confidence in the consistency of methods used. we have also investigated the crystalline quality of MBE grown GaN films containing quantum dot defect filters on sapphire substrates by defect delineating chemical etching. A pit density, correlated to dislocation density, of ~ $3x10^7$ cm^{-2} was observed in the GaN films grown on the multiple GaN/AlN QD layers as the buffer. This value represents a dramatic reduction in the dislocation density as compared to the films without using any QD layers.

In the third part of the report we presented vertical geometry Schottky type GaN/AlGaN MQW UV photodetectors. Three different device structures having different barrier thickness were designed and investigated. A maximum peak responsivity achieved in our detectors is 0.054 A/W in a back illuminated geometry with rough sapphire back side. Our comparative measurements of the single and double side polished sapphire substrates indicate that using double side polished substrates we can increase the responsivity to a value as high as 0.12 A/W. It has been shown that the photocurrent was limited by tunneling through the barriers, which upon further optimization can lead to increased device performance. The spectral responsivity window can also be tuned to shorter wavelengths, off course considering the difficulties in growing, by reducing the quantum well thickness and increasing the Al mole fraction in the AlGaN barriers to

about 300 nm. Reduction in defect density in our novel MQW photodetectors by using QDs buffer layer would expect to improve overall performances, further.

8. Publications resulting from this grant

1. A. Neogi, H. O. Everitt, H. Morkoç, T. Kuroda, and A. Tackeuchi "Enhanced radiative efficiency in GaN Quantum Dots grown by molecular beam epitaxy", IEEE Trans. on Nanotechnology, (2002).Neogi and H. Everitt,H. Morkoç M. Kuball T. Kuroda and A. Tackeuchi, "Size dependence of carrier recombination efficiency in GaN Quantum Dots" Electronics Letts, pending,

3. A. Neogi, H. Everitt, H. Morkoç, T. Kuroda, and A. Tackeuchi, "Time-resolved photoluminescence characterization of GaN Quantum Dots grown by molecular beam epitaxy", Appl. Phys. Letts., pending,
4. A. Neogi and H. Everitt, M. Reshcnikov, D. Huang, H. Morkoç M. Kuball T. Kuroda and A. Tackeuchi, "Optical Characterization of GaN quantum dot structures in AlN grown by molecular beam epitaxy", J. Appl. Phys., in press.

5. S. K. Zhang' W. B. Wang, F. Yun, L. He, H. Morkoç, X. Zhou, M. Tamargo, and R. R. Alfano, "Back-illuminated Ultraviolet Photodetector Based on GaN/AlGaN Multiple Quantum Wells", Appl. Phys. Letts, pending,

6. S. K. Zhang, W. B. Wang, I. Shtau, F. Yun, L. He, H. Morkoç, X. Zhou, M. Tamargo, and R. R. Alfano, "Back-illuminated GaN/AlGaN Heterojunction Ultraviolet Photodetector with High Internal Gain", Appl. Phys. Letts, pending,

7. A. Teke, S. Dogan, F. Yun, M.A. Reshchikov, H. Le, X.Q. Liu, H. Morkoç, S. K. Zhang, W. B. Wang and R.R. Alfano, "GaN/AlGaN Back Illuminated Multiple Quantum Well Schottky Barrier Ultraviolet Photodetectors", Appl. Phys. Lett., pending

8. A. Teke, S. Dogan, H. Le, D. Huang, J. Spradlin, H. Morkoç , S. K. Zhang, W. B. Wang and R.R. Alfano, "p-GaN-i-GaN/AlGaN MQW-n-AlGaN Back Illuminated Ultraviolet Detectors" J. Electronics Materials, pending

9. D. Huang, M. A. Reshchikov, F. Yun, T. King, A. A. Baski, and H. Morkoç, "Defect reduction with quantum dots in GaN grown on sapphire substrates by molecular beam epitaxy" Appl. Phys.Letts, Vol. 80, No 2, pp. 216-218, (2002).

10. D. Huang, F. Yun, M. A. Reshchikov, D. Wang, H. Morkoç, D. L. Rode, L. A. Farina, Ç. Kurdak, K. T. Tsen, S. S. Park, and K. Y. Lee, "Hall mobility and carrier concentration in free-standing high quality GaN templates grown by hydride vapor phase epitaxy", Solid State Electronics **45**, 711 (2001).

11. D. Huang, P. Visconti, K. M. Jones, M. A. Reshchikov, F. Yun, A. A. Baski, T. King, and H. Morkoç, "Dependence of GaN polarity on the parameters of the buffer layer grown by molecular beam epitaxy", Appl. Phys. Lett. **78**, 4145 (2001).

12. P. Visconti, D. Huang, M. A. Reshchikov, F. Yun, T. King, A. A. Baski, R. Cingolani, C. W. Litton, J. Jasinski, Z. Liliental-Weber, and H. Morkoç, "Investigation of defects and polarity in GaN using hot wet etching, atomic force and transmission electron

microscopy and convergent beam electron diffraction", Physica Status Solidi (b) **228**, 513 (2001).

13. F. Yun, D. Huang, M. A. Reshchikov, T. King, A. A. Baski, C. W. Litton, J. Jasinski, Z. Litiental-Weber, P. Visconti, and H. Morkoç, "A comparative study of MBE-grown GaN films having predominantly Ga- or N-polarity", Physica Status Solidi (b) **228**, 543 (2001).

14. D. Huang, P. Visconti, M. A. Reshchikov, F. Yun, T. King, A. A. Baski, C. W. Litton, J. Jasinski, Z. Liliental-Weber, and H. Morkoç, "Polarity of GaN grown on sapphire by molecular beam epitaxy with different buffer layers", Physica Status Solidi (a) **188**, 571 (2001).

15. M. A. Reshchikov, D. Huang, F. Yun, L. He, D. C. Reynolds, S. S. Park, K. Y. Lee, and H. Morkoç, "Photoluminescence of GaN grown by molecular beam epitaxy on freestanding GaN template", Appl. Phys. Lett. **79**, 3779 (2001).

16. P. Visconti, D. Huang, M. A. Reshchikov, F. Yun, R. Cingolani, D. J. Smith, J. Jasinski, W. Swider, Z. Liliental-Weber, and H.Morkoç, "Investigation of defects and surface polarity in GaN using hot wet etching together with microscopy and diffraction techniques", Mat. Sci. Eng. B – Solid **93**, 229 (2002).

17. P. Visconti, D. Huang, F. Yun, M. A. Reshchikov, T. King, R. Cingolani, J. Jasinski, Z. Liliental-Weber, and H. Morkoç, "Rapid Delineation of Extended Defects in GaN and a Novel Method for Their Reduction", phys. stat. sol. (a) **190**, 5 (2002).

18. D. Huang, M. A. Reshchikov, P. Visconti, F. Yun, A. A. Baski, T. King, H Morkoç, J. Jasinski, Z. Liliental-Weber, and C. W. Litton, "Comparative study of Ga- and N-polar GaN films grown on sapphire substrates by molecular beam epitaxy", J. Vac. Sci. Technol. B, Nov.-Dec. issue, 2002, to be published.

Book Chapters

1. H. Morkoç, "Growth of III-Nitride semiconductors and their characterization", in "Wide Energy Bandgap Electronics", Eds. S. Pearton and F. Ren, World Scientific, in press,

2. D. Huang, M. A. Reshchikov and H. Morkoç, "Quantum Dots", Eds. E. Borovitskaya and M. S. Shur, World Scientific, Singapore 2002

Presentations

1. A. Neogi, H. Everitt, M. Reshnikov Reshichkov, D. Huang, H. Morkoç, M. Kuball, T. Kuroda and A. Tackeuchi, "Optical Characterization of Self-Assembled GaN/AlN quantum dots" APS March meeting 2002

2. D. J. Smith, D. Huang, M. A. Reshchikov, F. Yun, T. King, and H. Morkoç, and C. W. Litton, "Dislocation reduction with quantum dots in GaN grown on sapphire substrates by molecular beam epitaxy", Spring MRS meeting, April 2002, San Francisco, CA,

3. M. A. Reshchikov, D. Huang, F. Yun, H. Morkoç, and C. W. Litton, "Excitons bound to structural defects in GaN", Fall 2001 Materials Society Meeting, November 2001,Boston, USA

4. D. Huang, C. W. Litton, M. A. Reshchikov, F. Yun, T. King, A. A. Baski, and H. Morkoç, "Improvement in Crystal Quality of GaN Films with Quantum Dots as Buffer Layers Grown on Sapphire Substrates by Molecular Beam Epitaxy", International Symposium on Compound Semiconductors, Sept. 2001, Japan

5. D. Huang, P. Visconti, M. A. Reshchikov, F. Yun, T. King, A. A. Baski, C. W. Litton, and H. Morkoç, "Dependence of GaN polarity on the parameters of the buffer layer grown by molecular beam epitaxy" International Conference on Nitride Semiconductors, July 2001 Denver CO USA.,

6. Hadis Morkoç "Growth of GaN/AlGaN Modulation Doped and Quantum Well Structures and the Associated Polarization effects", International Conference on Silicon Carbide and Related Materials, October 10-15, 1999, Research Triangle Park, NC. The proceedings papers is by Hadis Morkoç, M. A. Reshchikov, A. Baski, and M. I. Nathan, "GaN Quantum Dots on Sapphire and Si substrates" Proceedings of the International Conference on Silicon Carbide and Related Materials, October 10-15, 1999, Research Triangle Park, NC USA. Materials Science Forum, Trans Tech Publications, Vol. 338-342 - Part 2, pp. 1453-1458, 2000, eds. C. H. Carter, Jr., R. P. Devaty, and G. S. Rohrer.

7. M.A.Reshchikov, J. Cui, F.Yun, P.Visconti, M. I. Nathan, R. Molnar, and H. Morkoç "Growth and investigation of GaN/AlN quantum dots" Fall MRS, 2000,

9. Biography of the PI, Hadis Morkoç

Founders Professor of Department of Electrical Engineering with joint appointment in Physics Virginia Commonwealth University, Richmond, VA 23284-3072
Ph: 804-827-3765, Fax: 828-4269, hmorkoc@vcu.edu

Education

Ph.D. in Electrical Engineering, Cornell University, 1975
M.S. in Electrical Engineering, Istanbul Technical University, 1969
B.S. in Electrical Engineering, Istanbul Technical University, 1968

Professional Experience

1997-present	Founders Professor of Electrical Engineering with joint appointment in Physics, Virginia Commonwealth University
1995 – 1998	University Resident Research Professor, Wright Laboratory, Wright Patterson Air Force Base, OH.
1978 – 1997	Assistant and Associate Professor of Electrical Engineering and Research Associate Professor of Coordinated Science Lab, Univ. of Illinois, Urbana-Champagne, IL.
1987 – 1988	Distinguished Visiting Scholar, Jet Propulsion Laboratory and California Institute of Technology, Pasadena, CA.
1986 – 1997	Graduate Faculty, Dept. of Physics and Material Science, Univ. of Illinois
1978 – 1979	Resident Member of Technical Staff, AT&T Bell Laboratories.
1976 – 1978	Technical Staff, Central Research Laboratories, Varian Associates, Palo Alto, CA.

Professional Activities and Awards

Fellow: Inst. of Electrical and Electronics Engineers (IEEE), American Association for Advancement of Science (AAAS), American Physical Society (APS), Eta Kappa Nu; Life member: Sigma Xi, Phi Kappa Phi, Sigma Pi Sigma; Listed in Who is Who in America, Who's Who in the Midwest, American Men and Women in Science, Who's Who in Engineering, and Intl. Men of Achievement.

Publications

Some 1050 publications, 37 book chapters, 43 review & popular articles, and 3 books. Ranked 19th among 517,111 physicists in citations and impact between 1981 and 1997. Only the books, book chapters and tutorial reviews are listed below.

Books

1. H. Morkoç, H. Ünlü and G. Ji, "Fundamentals and Technology of MODFETs," Volume I, (Wiley and Sons, Wiley, Chichesters, West Sussex, UK (1991).

2. H. Morkoç, H. Ünlü and G. Ji, "Fundamentals and Technology of MODFETs," Volume II, (Wiley and Sons, Wiley, Chichesters, West Sussex, UK (1991).

3. H. Morkoç, "Nitride Semiconductors and Devices", Springer Verlag 1999. ISSN 0933-033x, ISBN 3-540-64038

4. H. Morkoç, Editor, A three volume book entitled "Recent and Evolving Advanced Semiconductor and Organic Nano-technologies": Vol.1 "Nanoscale Electronics for Computers and Optoelectronics for Telecommunications", Vol. 2. "Tunable and Photonics Band-gaps and Nano-tubes", Vol. 3. "Physics and Technology of Molecular and Biotech Systems" Academic Press, in preparation

Editor

1. R.L. Gunshor and H. Morkoç, Eds., "Growth of Compound Semiconductors," *Proc. of SPIE*, Bay Point, FL. Meeting, 1987.

2. F. Leonberger, H.C. Lee, F. Cappasso and H. Morkoç, Eds., *Proc. of 1987 OSA Picosecond Electronics and Optoelectronics Meeting*, Springer Verlag. Springer-Series in Electronics and Photonics, 24, Berlin Heidelberg, 1987.

3. G. Pensl, H. Morkoç, B. Monemar and E. Janzén, " Proceedings of the International Conference on Silicon Carbide, III-Nitrides and Related Materials, ICSC III-N, '97, Stockholm, Sweden, Aug. 31, 1997, Materials Science Forum, Vols. 264-268, Trans Tech Publication Ltd. ISSN 0255-5476

Special issues

1. H. Morkoç, Editor, *J. Vac. Sci. Technol. B*, Vol. 1, pp. 119-205, 1983.

2. . H. Morkoç and M. Abe, Editors, "Heterojunction Field Effect Transistors," *IEEE Trans. Electron. Dev.*, Vol. ED-33(5), pp. 541-792, 1986.

Book Chapters & Special Issues

1. H. Morkoç, "Modulation Doped $Al_xGa_{1-x}As$/GaAs Field Effect Transistors (MODFETs)," *Analysis, Fabrication and Performance, MBE and Heterostructures*, Eds. L.L. Chang and K. Ploog, Martinus Nijhoff Publishers, The Netherlands, Series E, Vol. 87, Ch. 7, pp. 625-676, 1985. (Based on a lecture given at NATO Advanced Series E, Study Institute on MBE and Heterostructures, March 7-19, 1983).

2. H. Morkoç, "Modulation Doped $Al_xGa_{1-x}As$/GaAs Heterostructors," in The *Technology and Physics of Molecular Beam Epitaxy*, Ed. E.H.C. Parker, Plenum, NY pp. 185-231, 1985.

3. H. Morkoç and H. Ünlü, "A Critical Discussion of Factors Affecting the Performance of MODFETs, Microwave and Digital Applications," in "*Device and Circuit Applications of III-V Semiconductor Superlattices and Modulation Doping*", Editor, R. Dingle, Semiconductors and Semimetals, Academic Press, 1987.

4. H. Ünlü and H. Morkoç, "Growth and Properties of GaAs-Based Devices on Si," in *GaAs Technology*, Vol. II, Ed. D.K. Ferry, Howard Sams and Co., Indianapolis, 1988. AFOSR.

5. R. Houdré and H. Morkoç, "Properties of MBE Grown GaAs on Si," *Critical Rev. Sol. State & Mat. Sci.*, Vol. 16(2), pp. 91-114, 1990. AFOSR.

6. H. Morkoç, "Strained Layers and Lasers in InGaAs/GaAs/AlGaAs Heterostructure System," *Presented at the NATO Advanced Research Workshop on Condensed Systems of Low Dimensionality*, Marmaris, Turkey, April 23-27, 1990, in Condensed Systems of Low Dimensionality pp. 579-612

7. H. Morkoç, "Strained Layer FETs, Lasers and Phototransistors in the InGaAs/GaAs/AlGaAs Heterostructure System," *in Proceedings of 1990 Seoul Int'l Symposium on the Physics of Semiconductors and Applications*, Seoul, Korea, August 20-21, pp 65 - 112, 1990.

8. S. Fang and H. Morkoç,"Lattice Mismatched Heteroepitaxy,in "*Integrated Optoelectronics*", Eds. M. Degenais, R.F. Leheney and J. Crow, Academic Press, San Diego, CA, pp. 145-209, 1995.

9. H. Morkoç, Editor, " Properties and Preparation of Emerging Device Heterostructures" Thin Solid Films, September 1993.

10. S. T. Strite and H. Morkoç, "Energetic Particle Assisted MBE," in S. Ismat Shah and D.A. Glocker, eds., *Handbook of Thin Film Process Technology*, IOP Publishing, Inc., in press.

11. H. Morkoç, "III-V Nitrides and Silicon Carbide for Photonic Materials and Devices," in "*CRC Handbook* of Photonics", pp. 49-84, , Boca Rotan, NY, 1997,M.S. Gupta, ed.

12. Samuel Strite and Hadis Morkoç, "Recipe for the MBE Growth of GaAs/Ge Heterostructures," in Handbook of Thin Film Process Technology Edited by D. Glocker and S. I. Shah Published by Institute of Physics Publishing, 1995. pp. X2.1:1-5.

13. A. Botchkarev, A. Salvador, B. Sverdlov, and H. Morkoç, "Recipe for GaN growth procedure by MBE" in Handbook of Thin Film Process Technology Edited by D. Glocker and S. I. Shah Published by Institute of Physics Publishing, ONR and AFOSR.

14. G. B. Gao, S. N. Mohammad, G. M. Martin, and H. Morkoç, "III-V Compound Semiconductor Heterojunction Bipolar Transistors", in "International Journal of High Speed Electronics and Systems", in "Compound Semiconductor Electronics: The Age of Maturity" Ed. M. S. Shur, World Scientific Publishing Company. ISBN 981-02-2325, 1996, pp. 85-174

15. S. N. Mohammad and Hadis Morkoç, "MODFETs: Operation, Status and Applications", in "Compound Semiconductor Electronics: The Age of Maturity". Ed. M. S. Shur, World Scientific Publishing Company. ISBN 981-02-2325, 1996, pp. 25-84

16. K. Suzue, S. N. Mohammad, and H, Morkoç, " GaAs Based Modulation Doped Heterostructures, in Properties of III-V Superlattices and Quantum Wells, Ed. P. K. Bhattacharya, Institute of Physics, INSPEC Series.

17. A. Salvador and H. Morkoç, " Molecular Beam Epitaxial Growth and Impurity Levels of GaAs based Quantum Wells and Superlattices" Ed. P. K. Bhattacharya, Institute of Physics, INSPEC Series.

18. H. Morkoç, "Foreword" for "Properties of Group III-Nitrides" Ed. by James H. Edgar, Institute of Physics, INSPEC Series. 1995.

19. M.E. Lin, S. Strite and H. Morkoç, "The Physical Properties of AlN, GaN and InN," *in The Encyclopedia of Advanced Materials*, Eds. D. Bloor, M. C. Fleming, R. J. Brook, S. Mahajan, Senior Ed. R. W. Cahn, pp. 79-86, Pergamon Press, (1994).

20. S. Strite, M.E. Lin and H. Morkoç, "Recent Progress in the MBE Growth of III-V Nitride Semiconductors," *in The Encyclopedia of Advanced Materials*, Eds. D. Bloor, M. C. Fleming, R. J. Brook, S. Mahajan, Senior Ed. R. W. Cahn, pp. 1629-1636, Pergamon Press, (1994).

21. Samuel Strite and Hadis Morkoç, "MBE Growth of GaAs/Ge Heterostructures," in Handbook of Thin Film Process Technology, D. A. Glocker and S. I. Shah, Eds., (Institute of Physics, Philadelphia 1995) pp. X2.1:1-5.

22. B. H. Bairamov, T. Gant, M. Delaney, Yu E. Kitaev, M. V. Klein, D. Levi, H. Morkoç, and R. A. Evarestov, "Theoretical and Experimental Study of Raman Scattering in Short Period (GaAs)m(AlAs)n Superlattices", in "The Best of Russian Physics", M. Levinstein and M. Shur eds., ISBN 981-02-1579-7, (1995), pp. 202-207.

23. Hadis Morkoç, F. Hamdani, and Arnel Salvador, "Electronic and Optical Properties of III-V Nitride-based Quantum Wells and superlattices" in Gallium Nitride, Academic Press, Eds. J. Pankove and T. Moustakas, in the Semiconductors and Semimetals Series Vol. 50, pp. 193-254, (1997). Eds. R. K. Willardson and E. R. Weber.

24. Hadis Morkoç, "Beyond SiC! III-V Nitride Based Heterostructures and Devices" in SiC Materials and Devices, Ed. Y. S. Park, Academic Press, Willardson and Beer Series. Vol. 52, pp. 307-394, (1998).

25. G. Popovici, S. N. Mohammad and Hadis Morkoç, "Deposition and Properties of III-Nitrides by Molecular Beam Epitaxy" Group III Nitride Semiconductor Compounds: Physics and Applications" Ed. B. Gil, Clarendon Press. April 1998. Oxford ISBN 0-19-850159-5

26. G. Popovici and H. Morkoç, "Growth and Doping of, and Defects in III-Nitrides" in GaN and Related Materials II Optoelectronic Properties of Semiconductors and Superlattices" Vol. 7. Pp. 93-172, Ed. S. J. Pearton, Series Editor M. O. Manaresh, Gordon and Breach Science Publishers, Amsterdam 1999. ISSN 1023-6619.

27. Pierre Lefebvre, Bernard Gil, Jean Massies, Nicolas Grandjean and Mathieu Leroux, Pierre Bigenwald, and Hadis Morkoç, "Physics and Optical Properties of GaN-AlGaN Quantum Wells", in "III-Nitride Semiconductors-Optical Properties I", Edited by O. Manasreh and H. X. Jiang, pp. 249-282, 2002, ISBN1-56032-972-6

28. Hadis Morkoç, "Wurtzite GaN Based Modulation Doped FETs and UV Detectors", in "Handbook of Thin Film Devices", Ed. Morris Francombe, Academic Press, Chapter 5, pp. 193-216. 2000, ISBN 0-12-762870-3

29. Hadis Morkoç, "Recent Developments in Microelectronics and Optoelectronics: A connector to Bioelectronics?", "Science at the Turn of the Millennium" Wiley VCH, Ed. E. Keinan.

30. H. Morkoç, "Aluminum, Gallium and Indium Nitrides," in *"The Encyclopedia of Materials*: Science and Technology", Eds. D. Bloor, M. C. Fleming, R. J. Brook, S. Mahajan, Senior Ed. R. W. Cahn, 79-Elsevier Press, pp. 121-127, ISBN:0-08-0431526

31. D. Huang, M. A. Reshchikov and H. Morkoç, "Growth, Structures, and Optical Properties of III-Nitride Quantum Dots", in Selected Topics in Electronics and Systems", Volume 25, 2002, in "IJHSES Vol. 12, No. 1 (March 2002) ", Ed. M. S. Shur, World Scientific. NSF, ONR and AFOSR.

32. Hadis Morkoç, "Emerging Advances in Microelectronics, Optoelectronics and Bioelectronics", in Advanced Semiconductor and Organic Nanotechniques, Academic Press, Ed. H. Morkoç, in press, AFOSR, ONR, NSF

33. Hadis Morkoç, "GaN-Based Modulation Doped FETs and Heterojunction Bipolar Transistors" in Recent and Evolving Advanced Semiconductor and Organic Nano-technologies, Academic Press, Ed. H. Morkoç, in press, AFOSR, ONR, NSF

34. Hadis Morkoç, Aldo Di Carlo, and R. Cingolani, "GaN-Based Modulation Doped FETs" in "Low dimensional nitride semiconductors", edited by B.Gil, Oxford university Press, Oxford UK.,pp. 341-414, ISBN 0 19 850974 X AFOSR, ONR, NSF

35. H. Morkoç, "Growth of III-Nitride semiconductors and their characterization", in "Wide Energy Bandgap Electronics" Eds. S. Pearton and F. Ren, World Scientific, in press, AFOSR, ONR, NSF

36. K. Subba Ramaiah and H. Morkoç, "Growth and characterization of GaN on ZnO/sapphire" in "Properties, Processes and Applications of ZnO", IEE Publishing House in London, UK. July, 2002, Ed by C. W. Litton, D. C. Reynolds, and T. Collins, AFOSR, BMDO, ONR, NSF.

37. Hadis Morkoç and L. Liu, "GaN-Based Modulation Doped FETs and Heterojunction Bipolar Transistors", in "Nitride Semiconductors - Handbook on Materials and Devices" P. Ruterana, M. Albrecht and J. Neugebauer, Eds. Wiley 2002

Tutorial, Review and Popular Articles

1. H. Morkoç and P.M. Solomon, "The HEMT: A Superfast Transistor," *IEEE Spectrum*, Vol. 21(2), pp. 28-35, February 1984. (Invited)

2. H. Morkoç and P.M. Solomon, "MODFET - Superschennelle Transistoren," *Technische Runschau*, Vol. TR10(77), Jahrgang, pp. 74-79, March, 1985. (invited)

3.R. Fischer and H. Morkoç, "New High Speed (Al,Ga)As Modulation Doped Field Effect Transistors," *IEEE Circuits and Devices Magazine*, Vol. 1, pp. 35-38, 1985.

4. T.J. Drummond, W.T. Masselink and H. Morkoç, "Modulation Doped GaAs(Al,Ga)As Heterojunction Field Effect Transistors: MODFETs," *Proc. of IEEE*, Vol. 74(6), pp. 773-822, June 1986. Translated into Russian as well.

5. H. Morkoç, "Developments in the GaAs on Si Technology," *American Institute of Physics* , News Release, 1986.

6. G. Munns and H. Morkoç, "GaAs on Si: Progress and Opportunities," *Physics Today*, Vol. 40. p. S66, Physics News in 1986, January 1987, (invited).

7. H.Z. Chen, A. Ghaffari, H. Wang, H. Morkoç and A. Yariv, "Continuous Wave Operation of GaAs Lasers on Si Substrates," *Optic News*, Vol. 13, pp. 13, December 1987.

8. H.Z. Chen, J. Paslaski, A. Yariv and H. Morkoç, "GaAs/AlGaAs Lasers on Si Substrates and Their High Frequency Characteristics," *Industrial Research and Development*, pp. 61, January 1988.

9. H. Ünlü and H. Morkoç, "Strained Layer InGaAs/GaAs Quantum Wells and Their Applications to Ultra-High Frequency MODFETs," *Solid State Technology*, Vol. 31, pp. 83-87, March 1988.

10. H. Morkoç, H. Ünlü, H. Zabel and N. Otsuka, "GaAs on Si: A Review," *Solid State Technology*, Vol. 31, pp. 71-76, March1988.

11. H.Z. Chen, J. Paslaski, H. Morkoç and A. Yariv, "High Speed GaAs Lasers and Detectors on Silicon for Optical Interconnects," *Optic News*, Vol. 14, pp. 24-25, 1988.

12. S. Iyer, H. Morkoç, N. Otsuka and H. Zabel, "Molecular Beam Epitaxy of Gallium Arsenide on Silicon," *Comments on Condensed Matter Physics*, Vol. 15(1), pp. 1-50, 1989.

13. S. Fang, K. Adomi, S. Iyer, H. Morkoç, H. Zabel, C. Choi and N. Otsuka, "Gallium Arsenide on Silicon: Epitaxial Growth and Characterization," *J. Appl. Phys. Rev.*, Vol. 68, pp. R31-R58, 1990.

14. K. Adomi, J.I. Chyi, S.F. Fang, T.C. Shen, S. Strite and H. Morkoç, "MBE Growth of GaAs and Other Compound Semiconductors with Applications to Devices," *Thin Solid Films*, Vol. 205(2), pp. 182-212, 1991.

15. H. Morkoç, "MODFETs Reach New Heights with Cut-Off Frequencies over 400 GHz," *IEEE Circ. and Dev. Magazine*, Vol. 7, pp.14-20, November 1991.

16. D. Biswas and H. Morkoç, "A Safety System for Gas Source Molecular Beam Epitaxy," *III/Vs Review*, Vol. 4(6), pp. 20-24, 1991.

17. T.C. Shen, G.B. Gao and H. Morkoç, "Recent Developments in Ohmic Contacts to III-V Compound Semiconductors " *Journal of Vacuum Science and Technology,* Vol. B10, pp. 2113-2132, 1992.

18. S.T. Strite and H. Morkoç, "GaN, AlN, and InN: A Review", *Journal of Vacuum Science and Technology,* Vol. B10, pp. 1237-1266.(1992)

19. G.B. Gao, H. Morkoç and M.F. Chang "Heterojunction Bipolar Transistor Design for Power Applications," *IEEE Transactions on Electron Devices*, Vol. ED-39, pp. 1987-1997, 1992.

20. M.S. Ünlü and H. Morkoç, "Wavelength Selective Optical Logic," *Optics and Photonics News*, p. 30, December 1992.

21. H. Morkoç, B. Sverdlov and G.B. Gao, "Strained Layer Heterostructures and Their Applications to MODFETs, HBTs and Lasers,"*Proceeding of IEEE*, Vol. 81, No. 4, pp. 492-556, April, 1993.

H. Morkoç, "Strained Layer Hetero-structures and Their Applications to MODFETS, HBTs, and Lasers", Proc. of IEEE, Vol. 81, No. 12, PG 493, pp. 1786-1786 (December 1993).

H. Morkoç, "Properties and Preparation of Emerging Device Heterostructures- Preface". Thin Solid Films, Vol. 25, No. 1-2, Pr. 7R7, August 25 1993.

22. D. S. L. Mui, Z. Wang and H. Morkoç, "A Review of III-V Semiconductor Based Metal-Insulator-Semiconductor Structures and Devices," *Thin Solid Films*, 231(1-2), pp. 197-210, August 25, 1993. In Special Issue: "Properties and Preparation of Emerging Device Heterostructures" Ed. H. Morkoç.

23. S. Strite, M.E. Lin and H. Morkoç, "Progress and Prospects for GaN and the III-V Nitride Semiconductors,"*Thin Solid Films*, 231(1-2), pp. 197-210, August 25, 1993. Special Issue: "Properties and Preparation of Emerging Device Heterostructures" Ed. H. Morkoç.

24. G. L. Zhou and H. Morkoç, "Si/SiGe Heterostructures and Devices", *Thin Solid Films*, 231(1-2),pp. 125-142, August 25, 1993. Special Issue: "Properties and Preparation of Emerging Device Heterostructures" Ed. H. Morkoç.

25. H. Morkoç, S. Strite, G. B. Gao, M.E. Lin, B. Sverdlov, and M. Burns, "A Review of Large Bandgap SiC, III-V Nitrides, and ZnSe Based II-VI Semiconductor Structures and Devices," *J. Appl. Phys. Reviews*, Vol. 76, No. 3. pp. 1363- 1398 August (1994).

26. H. Morkoç and S. N. Mohammad, " High Luminosity Gallium Nitride Blue and Blue-Green Light Emitting Diodes", Science, Vol. 267, pp. 51-55, Jan. 6, 1995. INVITED.

27. G. B. Gao, S. N. Mohammad, G. M. Martin, and H. Morkoç, "III-V Compound Semiconductor Heterojunction Bipolar Transistors", in "International Journal of High Speed Electronics and Systems", Vol. 6, No. 1, March 1995. " Ed. M. S. Shur, World Scientific Publishing Company.

28.S. N. Mohammad, A. Salvador, and H. Morkoç, " Emerging GaN Based Devices" Proc. IEEE, Vol. 83, pp. 1306-1355, October 1995. INVITED

29. S. N. N. Mohammad and H. Morkoç, " Progress and Prospects of Group III-V Nitride Semiconductors", Progress in Quantum Electronics. Vol. 20, Numbers 5 and 6, pp. 361-525, (1996), a monogram.

30. Hadis Morkoç, "Dopant incorporation and Defects in, and Applications of III-V Nitrides and Related Semiconductors", Proc. of the 8th International Symposium on the Physics of Semiconductors and Applications, Oct. 21-22, 1996. Seoul Korea. Journal of the Korean Physical Society, S26-S51, 1997.

31. H. Morkoç, " The Global Wireless Web" IEEE Circuits and Devices Magazine, Vol. 13, pp. 32-40, March 1997

32. S. N. Mohammad and H. Morkoç, "Light Emitting Diodes" in Wiley Encyclopedia of Electrical Engineering and Electronics Engineering, Ed. J. Webster, Vol. 11,pp. 315-326, 1999 John Wiley and Sons, Inc. Publishers.

33. H. Morkoç, "Modulation Doped Field Effect Transistors" in Wiley Encyclopedia of Electrical Engineering and Electronics Engineering, Vol. 13, pp. 455-477, 1999 Ed. J. Webster, John Wiley and Sons, Inc. Publishers. AFOSR, ONR.

34. H. Morkoç, "Wurtzite GaN Based Heterostructures by Molecular Beam Epitaxy", IEEE J. Photonics and Quantum Electronics, Ed. Richard Miles and I. Akasaki, IEEE Selected Topics in Quantum Electronics, Vol. 4, No. 3. pp. 537-549, 1998.

35. H. Morkoç, Roberto Cingolani, Walter Lambrecht, Bernard Gil, H.-X Jiang and J. Lin, and D. Pavlidis "Spontaneous polarization and piezoelectric field in Nitride Semiconductor Heterostructures", Proc. of the 9th International Symposium on the Physics of Semiconductors and Applications, Nov. 6-7, 1998. Seoul Korea. Journal of the Korean Physical Society, Vol. 34, pp. S224-233, June 1999

36. H. Morkoç, "Wurtzite GaN Based Modulation Doped FETs and UV Detectors" Naval Research Review, Vol. 51, No. 1. pp. 28-45 (1999).

37. Hadis Morkoç and Roberto Cingolani, and Bernard Gil, "Polarization Effects in Nitride Semiconductors and Device Structures", Materials Research Innovations, Vol. 3, No. 2, pp. 97-106, August 1999.

38. Hadis Morkoç, Roberto Cingolani, and Bernard Gil, "Polarization Effects in Nitride Semiconductor Device Structures, and Performance of Modulation Doped Field Effect Transistors" Solid State Electronics, vol.43, no.10, pp.1909-1927, Oct. 1999

39. Bernard Gil, Pierre Lefebvre and Hadis Morkoç, "Strain effects in GaN epilayers" C.R.Acad.Sci. Paris, t.100, Series IV, pp1-10, 2000 The Compte Rendu à l'académie des Sciences) Michel Voos, editor.

40. Hadis Morkoç, Aldo Di Carlo and R. Cingolani, "GaN-Based Modulation Doped FETs and UV Detectors", Solid State Electronics, Volume 46, Issue 2 pp. 157-202, (2002)

41. H. Morkoç, "Comprehensive Characterization of Hydride VPE Grown GaN Layers and Templates" Material Science and Engineering Reports (MSE-R), Vol. 259, R33/5-6, pp. 1-73, 2001

42. Hadis Morkoç, "III-Nitride semiconductor growth by MBE: Recent issues", Journal of Material Science: Materials in Electronics (MEL), Vol. 12, pp. 677-695, 2001.